

Exact Limits of Inference in Coalescent Models

James E. Johndrow and Julia A. Palacios

*390 Serra Mall
Stanford, California, 94305*

e-mail: johndrow@stanford.edu, juliapr@stanford.edu

Abstract: Recovery of population size history from molecular sequence data is an important problem in population genetics. Inference commonly relies on a coalescent model linking the population size history to genealogies. The high computational cost of estimating parameters from these models usually compels researchers to select a subset of the available data or to rely on non-sufficient summary statistics for statistical inference. We consider the problem of recovering the true population size history from two possible alternatives on the basis of coalescent time data. We give exact expressions for the probability of selecting the correct alternative in a variety of biologically interesting cases as a function of the separation between the alternative size histories, the number of individuals, loci, and the sampling times. The results are applied to human population history. This work has significant implications for optimal design when the inferential goal is to test scientific hypotheses about population size trajectories in coalescent models with and without recombination.

1. Introduction

Estimation of historical effective population size trajectories from genetic data provides insight into how genetic diversity evolves over time. Availability of molecular sequence data from different organisms living today and from ancient DNA samples together with the development of evolutionary probabilistic models [30], has enabled reconstruction of effective population size trajectories of human populations over the past 300,000 years [8, 19], Ebola virus over the course of the 2014 epidemic in Sierra Leone [29] and Egyptian hepatitis C virus for over 100 years [11].

Until recently, inference of effective population size trajectories was limited by scarcity of molecular sequence data such as single nucleotide polymorphisms (SNPs) and microsatellites. The increase in the total amount of genetic data obtained at different time points from a large number of individuals over large genomic segments (loci), and the development of more realistic probabilistic models, has led to a situation in which computationally tractable statistical inference is only available from non-sufficient summary statistics such as the site frequency spectrum (SFS) [21], from small numbers of samples, or from short genomic regions [2, 9, 14, 15, 26]. Gao and Keinan [7] give an extensive list of methods.

Accurate detection of change points in the effective population size trajectory is of scientific relevance in many applications such as the timing and length of the human expansion out-of-Africa [7], and extinctions of large mammals at the end of the Pleistocene epoch often attributed to the depredations of humans [23]. Rather than studying the statistical properties of different estimators, we consider how increasing the amount of genetic data increases our ability to distinguish between alternative hypotheses about population history under different evolutionary models. We evaluate the ability to detect change points by asking what the lowest achievable error rate is for classification between alternative hypotheses about population history with different change points –the Bayes error rate. Calculation of Bayes error rates allows us to answer such questions without the need to rely on any particular estimator. We give exact expressions for the probability that the optimal procedure can identify the truth, given coalescence data. We study the effect of adding more sequences and more loci under the coalescent model with and without recombination and under different demographic scenarios.

2. Coalescent evolutionary models

The standard n -coalescent [13] is a generative model of molecular sequence of n individuals sampled at random from a population of interest. In the single-locus neutral model, observed variation is the result of a stochastic process of mutations along the branches of the sample’s genealogy; the genealogy is a timed bifurcating tree (Figure 1A) that represents the ancestral relationships among samples. When moving back in time, two individuals find a common ancestor (coalesce) in the past with rate inversely proportional to the effective population size $N(t)$. Initially, the standard (homogeneous) n -coalescent assumed constant population size $N(t) = N$ and that sequences were sampled at the same time ($t=0$). Assuming a global mutation rate μ , the parameter of interest is $\theta = 2N\mu$. The standard neutral coalescent has been extended to variable population size $N(t)$ [25], varying sampling times (heterochronous coalescent [4]), and to account for population structure [1] and recombination [10].

Formally, the coalescent with variable effective population size $N(t)$ [25] is an inhomogeneous Markov point process of $n - 1$ coalescent times denoted by x_{n-1}, \dots, x_1 . The process starts with n individuals (lineages) at fixed time $x_n = 0$ until x_{n-1} when two of the n lineages meet their most recent common ancestor. The process continues merging (coalescing) pairs of lineages until time x_1 when the remaining two lineages reach a common ancestor. The resulting realization is a genealogy with $n - 1$ coalescent times like the one depicted in Figure 1A. The conditional density of coalescent time x_{k-1} is

$$f(x_{k-1} | x_k, N(t)) = \frac{C_k}{N(x_{k-1})} \exp \left\{ - \int_{x_k}^{x_{k-1}} \frac{C_k}{N(t)} dt \right\}$$

where $C_k = \binom{k}{2}$ is the combinatorial factor depending on the number of possible ways that two lineages can coalesce given that there are k lineages, and $N(t)$ is the effective population size, a positive function of time. It follows that the complete likelihood is given by

$$\begin{aligned} L(x_1, \dots, x_n | N(t)) &= f(x_n) \prod_{k=n}^2 f(x_{k-1} | x_k, N(t)) & (2.1) \\ &= \prod_{k=n}^2 \frac{C_k}{N(x_{k-1})} \exp \left\{ - \int_{x_k}^{x_{k-1}} \frac{C_k}{N(t)} dt \right\} \end{aligned}$$

where again $x_n \equiv 0$ by definition.

In the coalescent model with recombination [10] looking backwards in time, lineages can either coalesce or recombine at a random position along the chromosome. When a lineage undergoes recombination, the lineage is split into two. The structure representing coalescent and recombination events is the ancestral selection graph (ARG). In the ARG, different chromosomal segments (loci) can have different genealogies and these genealogies are correlated (Figure 1B). McVean and Cardin [17] and Marjoram and Wall [16] introduced Markovian approximations to the ARG called SMC and SMC’ respectively. In the SMC, two genealogies at different segments separated by a recombination event are necessarily different, while in the SMC’, these two genealogies are not necessarily different. Figure 1B shows an example realization of the SMC or SMC’ process. In this paper, we analyze these approximations to the ARG from pairwise coalescent times. Derivation for larger sample sizes involve complicated likelihoods [19] that are beyond the scope of this manuscript.

For $n = 2$, let x^i denote the pairwise coalescent time at the i -th locus; and let J be the number of recombination events. In models with recombination, loci are contiguous chromosomal segments delineated by recombination, so we will also use J to represent the number of loci. Under the SMC process, the transition density from x^i to x^{i+1} , conditioned on a recombination event at locus $i + 1$ is

$$f_{SMC}(x^{i+1} | x^i) = \frac{1}{x^i} \int_0^{x^{i+1} \wedge x^i} \frac{1}{N(x^{i+1})} q_1(u, x^{i+1}) du, \quad (2.2)$$

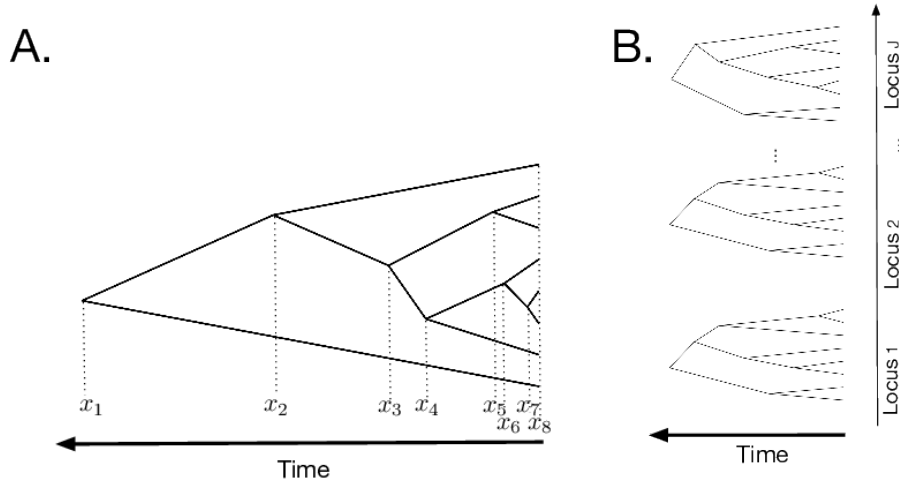


FIG 1. **A)** Genealogy of $n = 8$ sampled individuals. x_i is the time when two of $i + 1$ extant lineages coalesce. **B)** Multiple genealogies along a chromosomal region.

where

$$q_k(a, b) = \exp \left\{ - \int_a^b \frac{k dt}{N(t)} \right\}.$$

Given the current coalescent time x^i , a recombination breakpoint u is sampled uniformly along the height of the tree x^i . At time u , one of the two branches is pruned with equal probability, and a new coalescent time x^{i+1} is drawn with the standard coalescent rate.

Under the SMC' process, the transition density from x^i to x^{i+1} , conditioned on a recombination event at locus $i + 1$ is

$$f_{SMC'}(x^{i+1} | x^i) = \begin{cases} \frac{1}{x^i} \int_0^{x^i} \int_u^{x^i} \frac{1}{N(t)} q_2(u, t) dt du & \{x^{i+1} = x^i\} \\ \frac{1}{x^i N(x^{i+1})} \int_0^{x^{i+1}} q_2(u, x^{i+1}) du & x^{i+1} < x^i \\ \frac{1}{x^i N(x^{i+1})} q_1(x^i, x^{i+1}) \int_0^{x^i} q_2(u, x^i) du & x^{i+1} > x^i. \end{cases} \quad (2.3)$$

Given the current coalescent time x^i , a recombination breakpoint u is sampled uniformly along the height of the tree x^i . At time u , one of the two branches is selected with equal probability and split into two; one of the emanating branches follows the same trajectory back in time (old branch), while the other emanating branch can coalesce further back in time with any of the remaining two branches in the time interval (u, x^i) with rate $2/N(t)$. Conditional on failing to coalesce with any of the remaining branches in $[u, x^i]$, it coalesces with a branch emanating from the root at rate $1/N(t)$ at some time $x^{i+1} > x^i$. The old branch is then removed. When the new branch coalesces back with the old branch, the resulting tree is the same as the original tree with coalescent time x^i . This event corresponds to the first case in equation 2.3.

The likelihood under SMC is given by

$$L(x^1, \dots, x^J | N(t)) = \frac{1}{N(x^1)} \exp \left\{ - \int_0^{x^1} \frac{dt}{N(t)} \right\} \prod_{i=1}^{J-1} f_{SMC}(x^{i+1} | x^i),$$

and the likelihood under SMC' for $n = 2$ is obtained from the previous expression replacing f_{SMC} by $f_{SMC'}$.

3. Bayes error rates in the standard coalescent

We will start with the simple hypothesis testing setting in which the two hypotheses are:

$$\begin{aligned} H_1 : N(t) &= aN_0, & T \leq t \leq T + S \\ H_2 : N(t) &= bN_0, & T \leq t \leq T + S \end{aligned} \tag{3.1}$$

with $N(t)$ equal under H_1 and H_2 outside the interval $[T, T + S]$; a, b and S are positive constants and $T \geq 0$ (Figure 5). Our goal is to determine which hypothesis represents the true state of nature under which the data were generated. For simplicity of notation, we associate the state of nature with a parameter $\vartheta \in \{1, 2\}$ such that $H_1 : \vartheta = 1$ and $H_2 : \vartheta = 2$. A (binary) Bayes classifier or decision rule $\vartheta(x)$ has the form

$$\vartheta(x) = \begin{cases} 1 & \text{BF}_{12}(x) > 1 \\ 2 & \text{BF}_{12}(x) < 1 \\ \xi & \text{BF}_{12}(x) = 1 \end{cases}$$

where $\text{BF}_{12}(x)$ is the Bayes factor for H_1 vs H_2 , x is an observation of a random variable X , and $\xi \sim \text{Bernoulli}(1/2) + 1$. In the sequel, we drop the explicit argument and simply write BF_{12} in place of $\text{BF}_{12}(x)$. Thus, if $\vartheta(x)$ returns 1, we infer that the data were generated under H_1 , whereas if $\vartheta(x)$ returns 2, we infer that the data were generated under H_2 . In the case where each hypothesis is assigned prior probability of one half, the Bayes factor is exactly the likelihood ratio, and the probability of selecting H_1 is the probability that $\text{BF}_{12} > 1$ plus half the probability that $\text{BF}_{12} = 1$. In this case, the probability of correct classification is

$$\begin{aligned} \mathbf{P}[\vartheta(X) = \vartheta] &= \frac{1}{2} [\mathbf{P}(\log \text{BF}_{12} > 0 \mid H_1) + \frac{1}{2} \mathbf{P}(\log \text{BF}_{12} = 0 \mid H_1)] \\ &\quad + \frac{1}{2} [\mathbf{P}(\log \text{BF}_{12} < 0 \mid H_2) + \frac{1}{2} \mathbf{P}(\log \text{BF}_{12} = 0 \mid H_2)] \end{aligned}$$

When the prior is correct, the Bayes classifier is the optimal classifier, so that the probability of correct classification using the Bayes classifier is the maximum achievable probability. The Bayes error rate is $1 - \mathbf{P}[\vartheta(X) = \vartheta]$. As such, by studying the properties of the Bayes classifier, we obtain general limitations on inference for any classifier or test.

We first define some notation. Let $X = (X_1, X_2, \dots, X_{n-1})$ be the random vector of coalescent times with distribution given by (2.1). When multiple genealogies are available, we will denote the random variable corresponding to the collection of all J genealogies by X^J . Throughout, we abuse notation by writing $\mathbf{P}[\vartheta(X) = \vartheta]$ – or $\mathbf{P}[\vartheta(X^J) = \vartheta]$ when $J > 1$ – to represent the probability of correctly identifying the true state of nature.

The following theorems provide exact expressions for the probability of distinguishing between two hypotheses of the form 3.1 from pairwise coalescent data under the coalescent with variable population size (2.1).

Theorem 3.1. *Consider the simple hypothesis testing problem of the form 3.1 when a single pairwise coalescent time is observed ($n = 2$) and assign equal prior probabilities to both hypotheses. Then the probability of correctly distinguishing between the two hypotheses is:*

$$\mathbf{P}[\vartheta(X) = \vartheta] = \frac{1}{2} + \frac{1}{2} e^{-\Lambda(T)} \left(e^{-\frac{\delta \wedge S}{(a \vee b) N_0}} - e^{-\frac{\delta \wedge S}{(a \wedge b) N_0}} \right)$$

where

$$\delta \equiv \frac{abN_0}{b-a} \log \frac{b}{a} = \frac{abN_0}{a-b} \log \frac{a}{b} \geq 0,$$

and

$$\Lambda(T) \equiv \int_0^T \frac{1}{N(t)} dt.$$

Proofs of all results can be found in the Appendix. Type I and type II error rates can be obtained from the conditional probability expressions derived in the proof, and by modifying our proof to consider a classifier that thresholds $\text{BF}_{12}(x)$ at $\zeta(\alpha)$ for which $\mathbf{P}[\text{BF}_{12}(X) > \zeta(\alpha) \mid H_1] = 1 - \alpha$, one can perform power calculations for testing at level α where H_1 is designated as the null. We mention this as an obvious extension of our results, but do not pursue power calculations in the current work.

We now extend our previous result to the case when J independent genealogies from (2.1) are available. When multiple loci or chromosomal segments are either coming from different chromosomes or from the same chromosome at distant locations, genealogies at those locations can be assumed to be independent. When $n = 2$ and J independent genealogies with likelihood (2.1) are available, the sample configuration $L = (L_1, L_2, L_3)$ of the $J = L_1 + L_2 + L_3$ pairwise coalescent times is $L \sim \text{Multinomial}(J, \mathbf{p} = (p_1, p_2, p_3))$, where L_1 is the number of pairwise coalescent times that fall in the interval $(0, T)$, L_2 is the number of pairwise coalescent times that fall in the interval $[T, T + S]$, L_3 is the number of pairwise coalescent times that are greater than $T + S$, and

$$\begin{aligned} p_1 &= \mathbf{P}[X \leq T] = 1 - e^{-\Lambda(T)} \\ p_2 &= \mathbf{P}[T < X \leq T + S] = e^{-\Lambda(T)} - e^{-\Lambda(T+S)} \\ p_3 &= \mathbf{P}[X > T + S] = e^{-\Lambda(T+S)}. \end{aligned}$$

For this setting we have the following result

Theorem 3.2. *Consider the simple hypothesis testing problem of the form (3.1) when J independent pairwise coalescent times are observed ($n = 2$, $J \geq 1$). The probability of correctly distinguishing between the two hypotheses is*

$$\begin{aligned} \mathbf{P}[\vartheta(X^J) = \vartheta] &= \frac{1}{2} \mathbf{P}(L_2 = 0 \mid H_1) + \frac{1}{2} \sum_{(\ell_2, \ell_3): \ell_2 > 0} \mathbf{P}(L = \ell \mid H_1) \mathbf{P}[W^*(\ell_2) > \ell_2 \delta - \ell_3 S \mid H_1, L = \ell] \\ &\quad + \frac{1}{2} \sum_{(\ell_2, \ell_3): \ell_2 > 0} \mathbf{P}(L = \ell \mid H_2) \mathbf{P}[W^*(\ell_2) < \ell_2 \delta - \ell_3 S \mid H_2, L = \ell] \end{aligned}$$

where $W^*(\ell_2) = \sum_{j=1}^{\ell_2} X_*^j$ is the sum of ℓ_2 independent truncated coalescent times $X_*^j \in [0, S]$, each exponentially distributed with rate $(aN_0)^{-1}$ under H_1 , and rate $(bN_0)^{-1}$ under H_2 ; δ is defined as in Theorem 3.1, and

$$\ell \in \left\{ \ell = (\ell_1, \ell_2, \ell_3) : \ell_j \in \mathbb{N}, \sum_j \ell_j = J \right\}.$$

is an element of the support of $\text{Multinomial}(J, \mathbf{p} = (p_1, p_2, p_3))$.

To obtain numerical results, we approximate the distribution function $\mathbf{P}[W^*(\ell_2) < t]$ by Monte Carlo. In the next section we apply these results to the problem of distinguishing between two hypotheses about the human expansion out-of-Africa.

4. Human expansion out-of-Africa

Many of the statistical methods proposed over the last 15 years to infer effective population sizes from genetic data have been applied to human whole genomes [15, 22, 24, 19, 28]. Several studies agree that

non-African populations have experienced two severe bottlenecks, one attributed to the expansion out-of-Africa and the other attributed to the separation of Asian and European populations. There is, however, disagreement in the timing and length of such events.

Figure 2A shows a population history compatible with a human population history recovered from autosomal DNA in standard coalescent units [15]. In order to convert coalescent parameters into real time and size, time and $N(t)$ need to be divided by the mutation rate per generation. Times need be further multiplied by the generation time. To make our results comparable to previous studies [15, 12], we will assume a generation time of 25 years and that effective population size is expressed in units of 2.732×10^4 . That is, one unit in the y-axis of Figure 2A corresponds to 2.732×10^4 and one unit in the x-axis of the same plot corresponds to 68.3×10^4 years. In our analysis, we compare a population trajectory whose second bottleneck starts at time $T = 102.45\text{kya}$ (0.15 in standard units) versus a population trajectory whose second bottleneck starts earlier at time $T + S$ with S ranging from 30kyr to 150kyr. Our results from theorem 3.2 are depicted in Figure 2B. In order to correctly differentiate between the two hypotheses with $S = 130\text{kyr}$ with probability of at least 0.95, we need at least 35 loci. A correct classification with probability of at least 0.95 is achievable with at least 50 loci when $S = 60\text{kyr}$, that is, when the bottleneck started around 162kya versus 102kya.

Our results differ from previously published bounds based on coalescent Bayes error rates. Kim et al. [12] indicate that the minimal J such that any classifier can distinguish between H_1 and H_2 with probability at least 0.95 and $S = 130\text{kyr}$ is at least $J = 10$; while for $S = 60\text{kyr}$ it is $J \approx 20$. A detailed analysis of the differences between our results and previously published bounds of [12] – which reflect the fact that we give exact expressions instead of upper bounds on $\mathbf{P}[\vartheta(X^J) = \vartheta]$ – can be found in section 8.

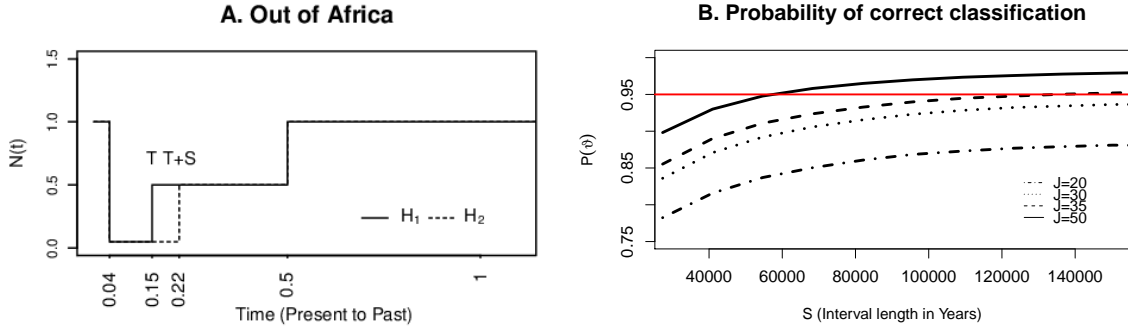


FIG 2. **A.** Human population history in coalescent units compatible with previous findings from whole genomes [15]. **B.** Probability of correct classification $\mathbf{P}[\vartheta(X^J) = \vartheta]$ as a function of the interval length S in years for several values of J loci corresponding to the two hypotheses depicted in A. Red line indicates probability of 0.95.

4.1. Value of incorporating ancient samples

Thus far, we have not considered the effect of incorporating samples at different sampling times, and have implicitly assumed that all samples are obtained at present. Results from Theorems 3.1 and 3.2 can be directly applied for the case when the two samples are obtained some time in the past. In particular, we assess the change in $\mathbf{P}[\vartheta(X^J) = \vartheta]$ when samples are obtained at the end of the bottleneck event at 102.45kya and when samples are obtained at 50kya. These scenarios are equivalent to putting $\Lambda(T) = 0$ and $\Lambda(T) = 1.54$, respectively. Ancient DNA (aDNA) corresponding to $T = 50\text{kya}$ is available from ancient genomes [5]. Obtaining data from the population immediately after the end of the event of interest is in some sense the optimal strategy for statistical inference on that event, and can have an enormous positive effect on inference. This is made clear by Figure 3A, which shows $\mathbf{P}[\vartheta(X^J) = \vartheta]$ for $J = 2, 3, 5, 10, 15$. For all but $J = 2$, $\mathbf{P}[\vartheta(X^J) = \vartheta] \geq 0.95$ can be

achieved for S greater than about 115kyr. For $J = 15$, it is possible to achieve $\mathbf{P}[\vartheta(X^J) = \vartheta] \geq 0.95$ with S larger than about 15kyr. When the samples are available from 50kya, it is possible to achieve $\mathbf{P}[\vartheta(X^J) = \vartheta] \geq 0.95$ with at least $J = 20$ loci.

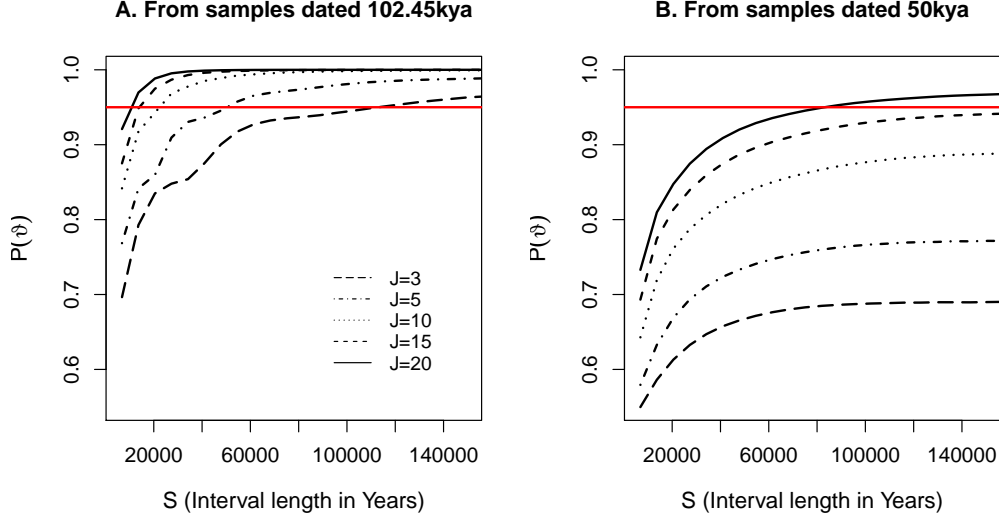


FIG 3. *Value of incorporating ancient samples.* Probability of correct classification $\mathbf{P}[\vartheta(X^J) = \vartheta]$ as a function of S in years for the human bottleneck example when samples are obtained before the bottleneck (A) and when samples are obtained around 50kya (B). Curves for different number of loci (J) is indicated by the line patterns. Red line indicates probability of 0.95.

5. Increasing the number of samples

Now we consider the case where $n > 2$. The following theorem gives an exact expression for the probability of correct classification in (3.1) from a single locus ($J = 1$) when $n = 3$.

Theorem 5.1. *Consider the simple hypothesis testing problem of the form 3.1 when a single genealogy of $n = 3$ individuals is observed. Define δ as in theorem 3.1, then the success rate of the optimal classifier is*

$$\mathbf{P}[\vartheta(X) = \vartheta] = \frac{1}{2} + \frac{1}{4}e^{-3\Lambda(T)}\xi(a, b, N_0, T, S)$$

where

$$\begin{aligned} \xi(a, b, N_0, T, S) &= 3e^{2\Lambda(T)} \left[e^{-\frac{\delta\Lambda S}{aN_0}} - e^{-\frac{\delta\Lambda S}{bN_0}} \right] \\ &+ 3 \left[e^{-\frac{2(0\vee(\frac{\delta-S}{2}\wedge S))+S}{aN_0}} - e^{-\frac{2(0\vee(\frac{\delta-S}{2}\wedge S))+S}{bN_0}} \right] - 3 \left[e^{-\frac{\delta\Lambda S}{aN_0}} - e^{-\frac{\delta\Lambda S}{bN_0}} \right] \\ &+ \begin{cases} 0 & S < \frac{2}{3}\delta \\ e^{-\frac{2\delta}{bN_0}} \left(1 + \frac{2\delta-3S}{bN_0} \right) - e^{-\frac{2\delta}{aN_0}} \left(1 + \frac{2\delta-3S}{aN_0} \right) & \frac{2}{3}\delta < S < 2\delta \\ e^{-\frac{2\delta}{aN_0}} \left(\frac{4\delta}{aN_0} + 2 \right) + e^{-\frac{2\delta}{bN_0}} - 3e^{-\frac{T-2\delta-S}{bN_0}} + e^{-\frac{2\delta+S}{bN_0}} \frac{3T-3S-4\delta}{bN_0} & S > 2\delta \end{cases} \end{aligned}$$

The proof is located in Appendix C. We can use this result to assess how much an additional sample helps in identifying the true population size history. Figure 4 shows four examples of $\mathbf{P}[\vartheta(X) = \vartheta]$ as a function of a while fixing $b = 1$; increasing a is equivalent to increasing the separation between the two hypothetical population size histories. In two of the examples, $N(t) = 1$ outside the interval $[T, T + S]$, and in the other two $N(t) = e^t$ outside this interval. In both cases, the probability of identifying the true effective population size function is considerably higher with $n = 3$ than $n = 2$ when $|a - b|$ is not too close to zero. Thus, additional coalescent times can help considerably to distinguish between alternative histories.

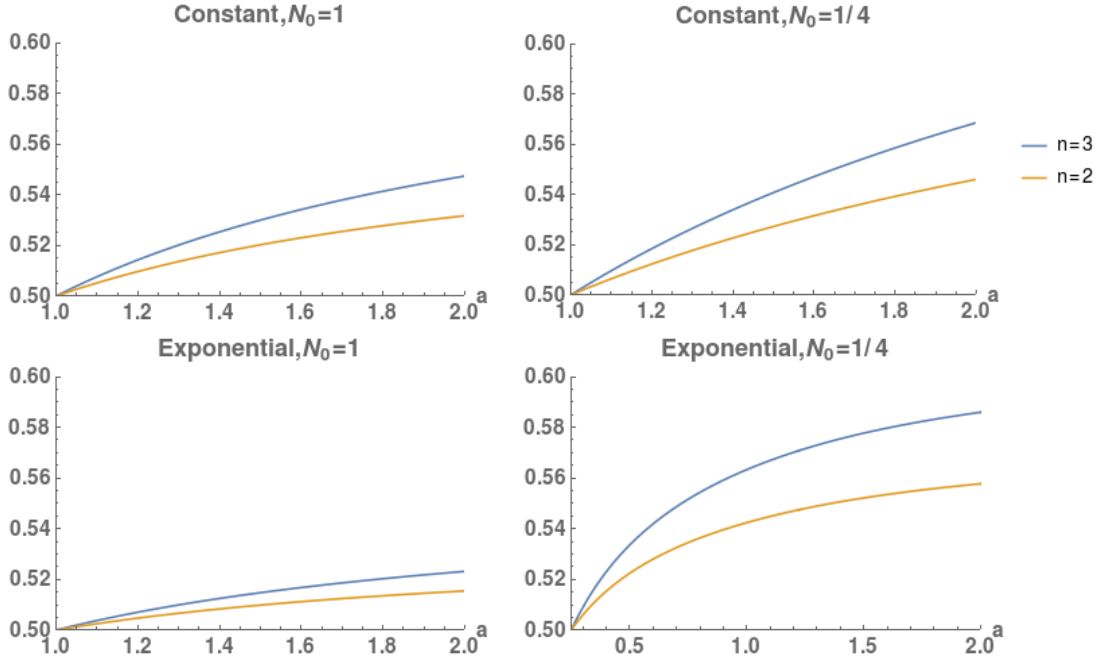


FIG 4. *Effect of adding an additional sample.* Probability of correct classification $\mathbf{P}[\vartheta(X) = \vartheta]$ as a function of a for classification problem 3.1. In each case we put $T = 1$, $S = 1/2$, and $b = 1$. We compare the effect of adding one more sample ($n = 2$ vs $n = 3$) for constant and exponential growth population trajectories.

It is clear from the proof of Theorem 5.1 that while it is possible to obtain exact expressions for $n > 3$, the number of cases that must be treated will grow exponentially in n . Of course, it is still possible to approximate $\mathbf{P}[\vartheta(X) = \vartheta]$ by simulation for arbitrary n . Here, we re-analyze the out-of-Africa classification problem considered in Section 4 for $n = 10$ and $J = 1, 5, 10, 20$ as a function of interval length S and compare to $n = 2$. The value of $\mathbf{P}[\vartheta(X^J) = \vartheta]$ is approximated by 10,000 Monte Carlo samples. Results are shown in Figure 5. In contrast to the case of $n = 2$, where $J = 50$ was required to achieve $\mathbf{P}[\vartheta(X^J) = \vartheta] = 0.95$ for $S = 60\text{Kyr}$, when $n = 10$ it is possible to achieve the same success probability with $J = 20$. Thus, increasing the number of contemporaneous sequences or loci gives sharper inference on the duration of the expansion out-of-Africa.

6. Bayes error rates in the sequentially Markov coalescent

We now consider the same classification problem as in (3.1) from J consecutive loci along a chromosomal region. We assume the ideal scenario in which we observe the J pairwise coalescent times ($n = 2$) corresponding to each of these J loci separated by $J - 1$ recombination events. Further, we assume that effective population size trajectories under H_1 and H_2 are piece-wise constant functions

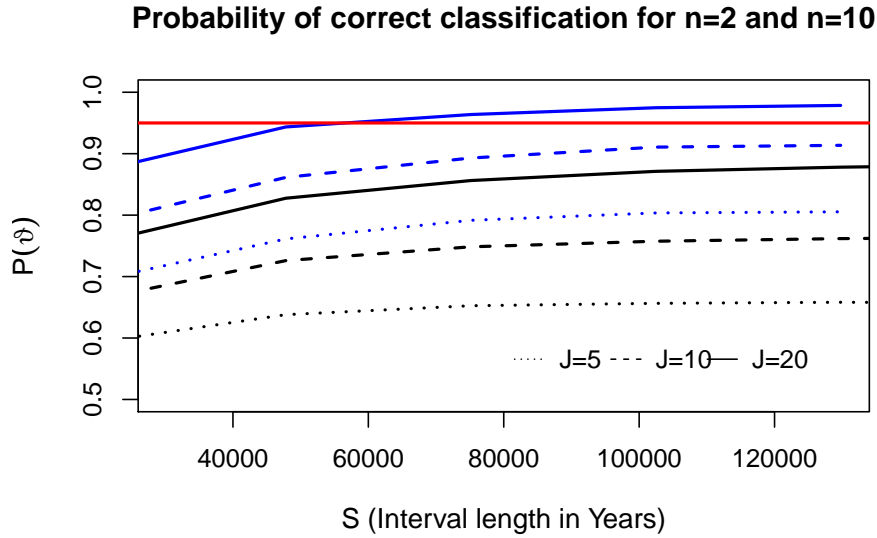


FIG 5. *Effect of adding more samples in the out-of-Africa scenario* Blue lines represent $\mathbf{P}[\vartheta(X) = \vartheta]$ as a function of bottleneck length S for $n = 10$ and black lines represent $\mathbf{P}[\vartheta(X) = \vartheta]$ for $n = 2$. Different number of loci are distinguished by line patterns. Red line indicates probability of 0.95.

over time such as the out-of-Africa scenario in Figure 2A. We then approximate $\mathbf{P}[\vartheta(X^J) = \vartheta]$ by Monte Carlo from 10,000 simulations generated from each hypothesis under the two coalescent models with recombination: SMC (2.2) and SMC' (2.3).

We re-analyze the out-of-Africa classification problem considered in section 4 for $n = 2$ and $J = 2, 5, 10, 20, 30, 35$ as function of interval length S under independent loci (3.2), SMC' (2.3) and SMC (2.2). We show that either under SMC' or independent loci, $\mathbf{P}[\vartheta(X^J) = \vartheta] = 0.95$ is achievable with $n = 35$ loci. For $J < 20$, the Bayes error rate in SMC is smaller than the other two alternatives. The significance of this is that it is not necessary to have many independently segregating loci to make inference on features of the historical population size. Instead, virtually the same number of non-independent loci separated by recombination events will suffice. The set of all dependent loci is of course considerably larger than the largest set of independent loci, so the result suggests optimism in the potential to reconstruct features of the population size trajectory in the relatively distant past.

7. Other scenarios

We now consider a more general classification problem when pairwise coalescent data is available at a single locus or multiple loci :

$$\begin{aligned} H_1 : N(t) &= N_1(t) \\ H_2 : N(t) &= N_2(t). \end{aligned} \tag{7.1}$$

We consider the case where $N_2(t) = cN_1(t)$ for $c \in (0, 1)$, where analytic expressions for $\mathbf{P}[\vartheta(X) = \vartheta]$ are available even when $N_1(t)$ is not piecewise constant.

Theorem 7.1. *Consider the simple hypothesis testing problem of the form (7.1) such that $N_2(t) = cN_1(t)$ with $0 < c < 1$ when a single pairwise coalescent time is observed ($n = 2$) and assign equal*

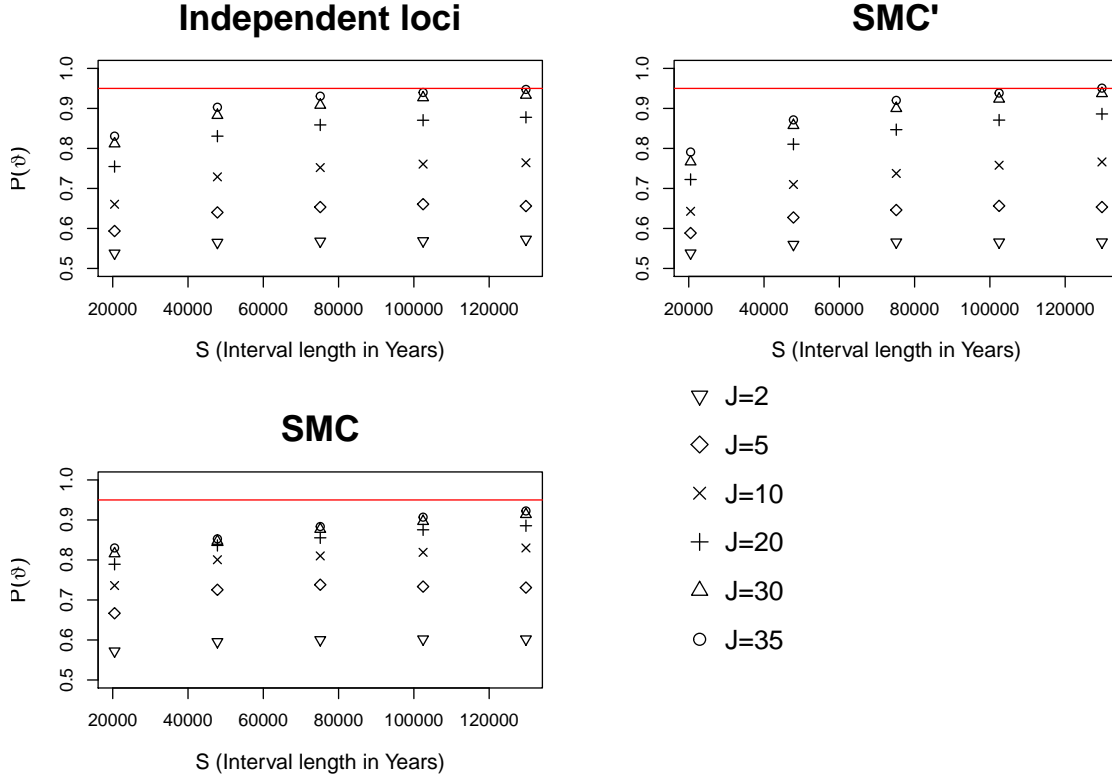


FIG 6. *Sequentially Markov coalescent in the out-of-Africa scenario* Probability of correct classification under independent sampling, SMC' and SMC. Different patterns represent different number of loci. Red line indicates probability of 0.95.

prior probabilities to both hypotheses. Then the probability of correct classification is:

$$\mathbf{P}[\vartheta(X) = \vartheta] = \frac{1}{2}c^{\frac{c}{1-c}} + \frac{1}{2}\left(1 - c^{\frac{1}{1-c}}\right).$$

Theorem 7.2. Consider the conditions of Theorem 7.1 for J independent loci. The probability of correct classification is

$$\mathbf{P}[\vartheta(X^J) = \vartheta] = \frac{1}{2}\left(1 - \frac{1}{\Gamma(J)}\left[\gamma\left(J, \frac{-Jc \log c}{1-c}\right) - \gamma\left(J, \frac{J \log c}{c-1}\right)\right]\right). \quad (7.2)$$

where $\gamma(a, b)$ is the lower incomplete gamma function.

Figure 7 shows (7.2) as a function of c for different values of J . As expected, the larger J , the larger the value of c at which high probability of identifying the true population size history can be achieved. However, even for $J = 100$, we must have $c \approx 0.75$ or smaller to give probability 0.95 of selecting the true population size history. Our results from Theorems 7.1 and 7.2 differ from previously published Bayes error rates bounds [12]. In the following section, we present a more detailed analysis of the differences between our exact expressions and the bounds [12].

8. Bounds on Bayes classification error.

Kim et al. [12] provided lower bounds on Bayes error rates from pairwise coalescent data. We now

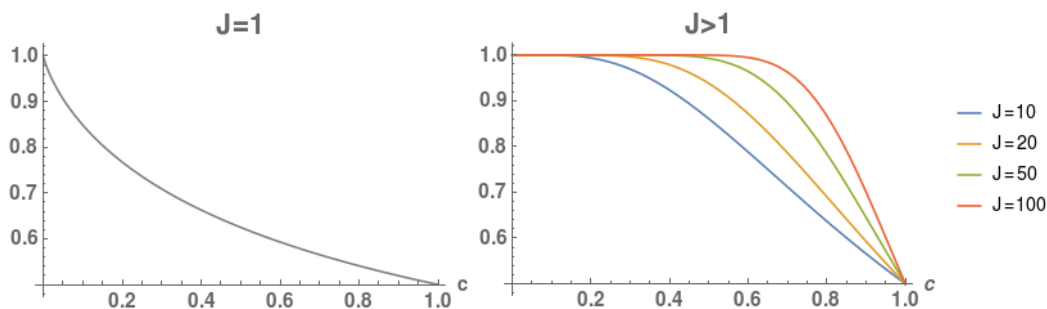


FIG 7. **Left.** Probability of correct classification $\mathbf{P}[\vartheta(X) = \vartheta]$ as in (7.2) when $N_2(t) = cN_1(t)$ and $J = 1$ (Theorem 7.1). **Right.** $\mathbf{P}[\vartheta(X^J) = \vartheta]$ as a function of c for several values of J .

provide a comparison of some of our results to these previously published bounds. In this section, we will let Y denote a random coalescence time generated under H_1 and Z denote a random coalescence time generated under H_2 . Assuming a classification problem of the form (3.1) and prior probability $1/2$ on H_1 and H_2 , the Bayes error rate for any classifier is at least $(1 - \Upsilon)/2$ where

$$\Upsilon = d_{\text{TV}}(Y, Z) = d_{\text{TV}}(\mu, \nu) \equiv \sup_A |\mu(A) - \nu(A)|$$

is the total variation distance between probability measures μ, ν , such that $Y \sim \mu, Z \sim \nu$. The authors then apply the inequality

$$\frac{1}{2}d_{\text{TV}}^2 \leq d_{\text{H}}^2$$

where d_{H} is the *Hellinger distance*. Let P and Q be probability measures that are absolutely continuous with respect to some dominating measure λ , and let $f_P = \frac{dP}{d\lambda}, f_Q = \frac{dQ}{d\lambda}$ be their respective Radon-Nikodym derivatives. The Hellinger distance between P and Q is defined by

$$d_{\text{H}}^2(P, Q) = \frac{1}{2} \int (\sqrt{f_P} - \sqrt{f_Q})^2 d\lambda.$$

In the case where λ is Lebesgue measure, f_P and f_Q are the densities of P and Q . The main result of [12] is

Theorem 8.1 (Kim et al. [12], Theorem 1). *Suppose $n = 2$ in (2.1). Then*

$$d_{\text{H}}^2(Y, Z) = e^{-\int_0^T \frac{1}{N(t)} dt} \left(1 - e^{-\frac{(a+b)S}{2abN_0}} \right) \frac{(\sqrt{a} - \sqrt{b})^2}{a + b}.$$

We give a proof in the appendix that fills in some additional details of the proof in [12]. Rather than obtaining bounds on the Bayes error rate using the Hellinger distance, we compute the probability of correct inference on ϑ .

In Figure 8, we compare our results to the Hellinger bounds of [12] for different values of a, b, N_0 . The upper bound based on the Hellinger distance from [12] is given by

$$\frac{1}{2} + \frac{1}{2} \sqrt{2H^2(f_1, f_2)}$$

with $H^2(f_1, f_2)$ as in (F.3). Evidently the Hellinger bound is quite loose when $|a - b|$ is not near zero.

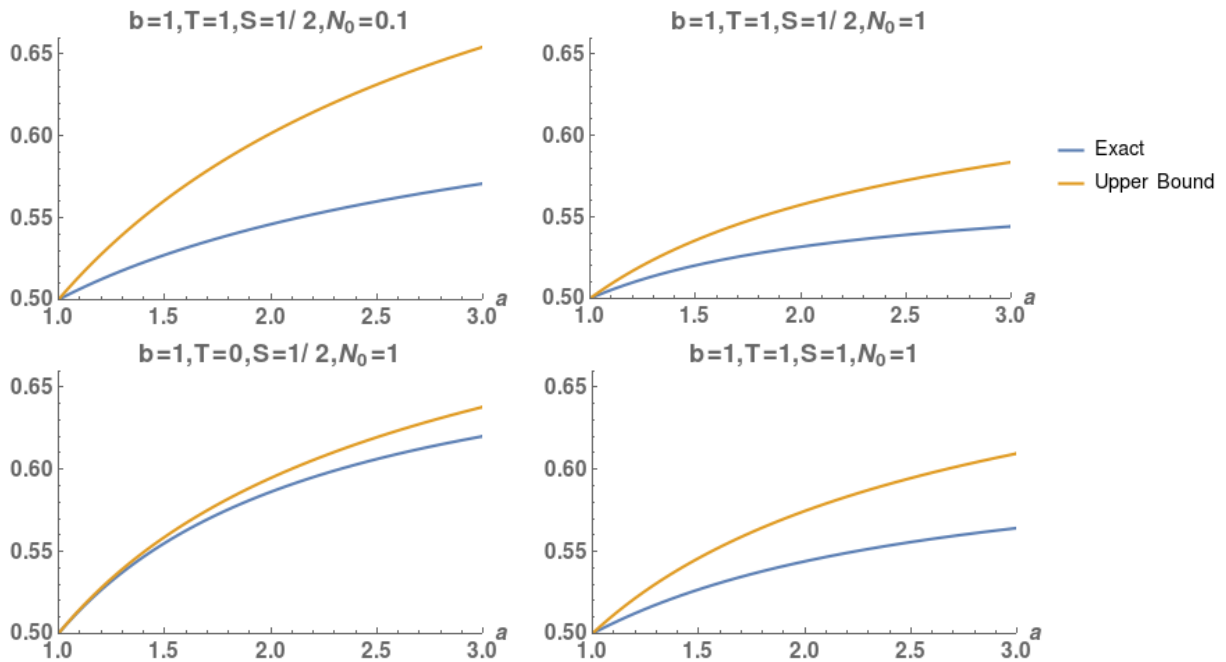


FIG 8. Exact $\mathbf{P}[\vartheta(X) = \vartheta]$ (blue) and upper bound on this quantity from [12] (yellow) for different values of $T, S,$ and N_0 .

Kim et al. [12] use the inequality

$$d_H^2(Y^J, Z^J) \leq J d_H^2(Y, Z), \tag{8.1}$$

which holds when the J genealogies are independent, in combination with Theorem 8.1, to obtain lower bounds on the error rate for J independent loci. They then use these lower bounds to calculate quantities like bounds on the minimal S such that the correct hypothesis will be selected with probability 0.95 for several examples. In contrast, our results give the exact value of $\mathbf{P}[\vartheta(X^J) = \vartheta]$, which allows us to compute exactly the value of S to achieve the desired Bayes error rate for any J . The results on the minimal number of loci J necessary to achieve a fixed error rate differ substantially from the results in [12]. The looseness of the bound on $\mathbf{P}[\vartheta(X^J) = \vartheta]$ obtained using the Hellinger distance is clear from Figure 8.

Moreover, the expression in (7.2) can be directly compared with Theorem 3.2 of [12]. Translated into our notation and conventions, this result states that

$$\mathbf{P}[\vartheta(X^J) = \vartheta] \leq \frac{1}{2} + \frac{1}{4} \sqrt{J(n-1)} \left(\frac{1}{c} - 1 \right). \tag{8.2}$$

Figure 9 shows the bound from (8.2) along with the exact probability of identifying the true $N(t)$ as a function of c for $n = 2$ and different values of J . The bound is apparently quite loose when c is not close to 1. It becomes trivial (greater than 1) for $c \approx 0.4$ when $J = 1$ and $c \approx 0.7$ when $J = 10$.

9. Bayes risk under conjugate priors

Although our focus has been on inferential limits for distinguishing among two states of nature, we briefly consider estimation of a constant population size trajectory. We assess the risk of estimators

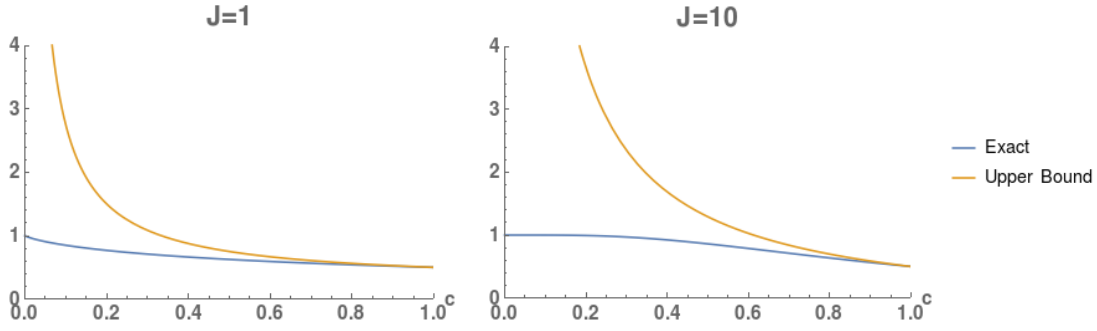


FIG 9. Exact $\mathbf{P}[\vartheta(X^J) = \vartheta]$ compared to the upper bound from Theorem 3.2 of [12] as a function of c for two different values of J .

of the function $\Lambda(x)$ in the case of $n = 2$ and $N(t) = \frac{1}{c}$ with conjugate priors on c . In this setting, the coalescent time x is $\text{Exponential}(c)$ with conjugate prior $c \sim \text{Gamma}(\alpha, \beta)$ and for a sample of J independent pairwise coalescent times we have

$$c \mid x^{(1)}, \dots, x^{(J)} \sim \text{Gamma}(\alpha + J, \beta + J\bar{x})$$

with posterior expectation

$$\mathbf{E}[c \mid x^{(1)}, \dots, x^{(J)}] = \frac{\alpha + J}{\beta + J\bar{x}}.$$

Note that

$$J\bar{X} \mid c \sim \text{Gamma}(J, c)$$

so the squared error risk of the Bayes estimator of c is

$$R(\hat{c}, c) := \int_0^\infty \left(\frac{\alpha + J}{\beta + z} - c \right)^2 \frac{\beta^\alpha}{\Gamma(\alpha)} z^{J-1} e^{-cz} dz.$$

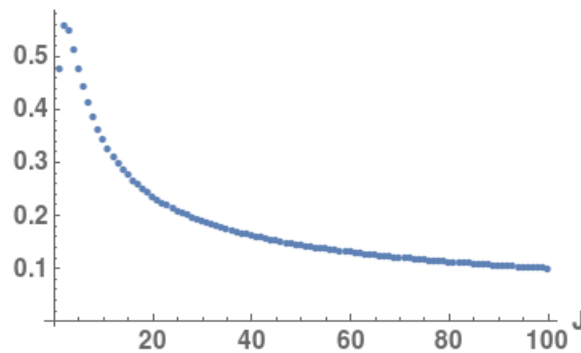
This can be evaluated in terms of analytic functions for any α, β , but for simplicity, we assume $\alpha = \beta = 1$, so that

$$\begin{aligned} R(\hat{c}, c) &= \int_0^\infty \left(\frac{1 + J}{1 + z} - c \right)^2 e^{-z} dz \\ &= c \left(-(J + 1)e^c (J^2 + (J + 3)c - 1) E_J(c) + (J + 1)^2 + c \right) \end{aligned}$$

where

$$E_J(c) = \int_1^\infty \frac{e^{-cz}}{z^J} dz,$$

is a generalization of the exponential integral function. Figure 10 shows the square root of risk as a function of the number of loci J for values of $J \in \{1, \dots, 100\}$ with $c = 1$. The root risk decreases logarithmically in J ; it is approximately 0.1 for $J = 100$, and about 0.24 for $J = 20$. Thus, if one wants the root risk to be small relative to the truth, it is necessary to have J rather large. In this example, in order to have the root risk be about 10 percent the magnitude of the truth, we need $J \approx 100$.

FIG 10. Root risk of Bayes estimator with $\alpha = \beta = 1$ and $c = 1$.

10. Discussion

Availability of ancient and present-day DNA samples from a population allows statistical reconstruction of the effective population size trajectory. The effective population size is a measure of relative genetic diversity whose actual magnitude is not easily interpreted in units of census population size [31]. However, changes of effective population size over time are informative about the genetic history of the population. In this manuscript, we assess the ability to differentiate or classify between alternative hypotheses about the effective population size.

Assessment of inferential limits in population genetic studies is becoming important in the face of ongoing large-scale studies of genetic variation. Statistical methods are usually restricted to small samples or rely on approximations and insufficient summary statistics. As such, choosing the optimal subset of data with which to perform statistical inference is of great interest. Aspects of the data and adequacy of the model will affect the ability to draw meaningful conclusions. Here, we have eliminated the effect of factors such as data quality, sample selection and sequence alignment and concentrated on the ideal scenario of having a complete realization of the genealogical process free of errors. In practice, genealogies are not available and instead we observe DNA sequence variation; therefore our results are upper bounds on the achievable probability of recovering the true population size history in population genetic studies. These results provide guidance to practitioners in choosing a sampling design subject to computational constraints. In particular, they give insight into the key questions of which scientific hypotheses can be assessed, and the optimal choice of the number of loci, sampling times, and individuals to include in a sample to achieve a specific inferential goal. They also offer a possible explanation for disagreement in the literature over timing and duration of historical genetic events such as the out-of-Africa human population bottleneck, suggesting that some studies may simply not have sufficient data to distinguish between the hypotheses of interest with high probability.

Fu and Li [6], Pluzhnikov and Donnelly [20], and Felsenstein [3] argued that in the constant population model ($\theta = 2N\mu$), accuracy of estimators of θ increases linearly in the number of independent loci, logarithmically in the number of samples, and is unaffected by sequence length. In the coalescent with variable population size, Myers et al. [18] showed that estimators based on the SFS cannot distinguish between two alternative hypotheses. Terhorst and Song [27] showed that estimators of $N(t)$, based on the same statistic SFS, have minimax rate of convergence that is logarithmic in the number of independent loci and independent of the number of individuals sampled. Our results support a more complex view of the value of additional samples or loci. While in general, the improvement in the probability of recovering the true population history appears to be sublinear in both J and n , the improvement from adding an additional sample or locus depends greatly on the details of the two hypotheses being considered. For example, increasing from $n = 2$ to $n = 3$

samples can in some cases double the excess probability of recovering the truth $\mathbf{P}[\vartheta(X) = \vartheta] - 1/2$ (the probability is always lower bounded by $1/2$). In general, smaller improvements are seen from increasing J , but we have demonstrated that high probability of recovering the true population size history in the out-of-Africa example is attainable using values of n and J that are available from modern datasets and for which exact computation is feasible. In addition, our results suggest that incorporation of ancient genomes is the optimal strategy to improve inferential performance in the expansion out-of-Africa problem, which is of significant interest in human population genetics.

Pluzhnikov and Donnelly [20] considered the constant population model with recombination and argued that when the recombination rate is high, increasing the sequence length effectively increases the number of independent loci. Indeed, when two genomic segments are separated by a recombination event, individuals at these two segments (loci) derive from two different but correlated genealogies. As the number of recombination events increases, the correlation between the two genealogies becomes weaker, and hence increasing the length of sequenced segments increases the opportunity to observe a larger number of realizations from genealogically independent loci [19, 10]. Our results for the pairwise SMC' model of recombination support the remarkable conclusion that loci separated by recombination events have nearly the statistical value as the same number of independent loci. This suggests that pairwise SMC' is a very powerful framework for inference of population size trajectories. An interesting future direction is to explore the effect of increasing the number of individuals in the SMC'.

Appendix A: Proof of theorem 3.1

Proof. Define

$$\Lambda(w, x) \equiv \int_w^x \frac{1}{N(t)} dt.$$

For shorthand we write $\Lambda(x) = \Lambda(0, x)$. $\Lambda : \mathbb{R}_+ \rightarrow \mathbb{R}_+$ is a monotone strictly increasing function, which is enough to guarantee the existence of an inverse

$$\Lambda^{-1}(t) = x \iff \Lambda(x) = t,$$

The likelihood ratio for H_1 vs H_2 (3.1) can be expressed by

$$\log \text{BF}_{12}(x) = \begin{cases} 0 & x < T \\ \log \frac{b}{a} - \frac{x-T}{aN_0} + \frac{x-T}{bN_0} & T \leq x < T + S \\ \frac{S}{bN_0} - \frac{S}{aN_0} & T + S \leq x \end{cases} \quad (\text{A.1})$$

Notice that the waiting time until the coalescent event has survival function

$$\mathbf{P}[X > x] = e^{-\Lambda(x)}.$$

Now we want to calculate $\mathbf{P}[\vartheta(X) = 1 \mid H_1]$. Assume that if $\log \text{BF}_{12}(x) = 0$ we select either H_1 or H_2 by flipping a fair coin. If $a > b$ then

$$\log \text{BF}_{12}(x) > 0, T \leq x \leq T + S \iff x > \delta + T,$$

and if $b > a$

$$\log \text{BF}_{12}(x) > 0, T \leq x \leq T + S \iff x < \delta + T.$$

Assuming $a > b$ and denoting $f_i(x)$ the density under H_i for $i = 1, 2$, we have

$$\begin{aligned} \mathbf{P}[\vartheta(X) = 1 \mid H_1] &= \frac{1}{2} \mathbf{P}[X < T \mid H_1] + \int_T^{T+S} \mathbf{1} \left\{ x > \frac{ab}{b-a} N_0 \log \frac{b}{a} + T \right\} f_1(x) dx \\ &\quad + \mathbf{1}\{b < a\} \mathbf{P}[X > T + S \mid H_1] \\ &= \frac{1}{2} (1 - e^{-\Lambda(T)}) + \int_{T+(\delta \wedge S)}^{T+S} e^{-\Lambda(T)} \frac{1}{aN_0} e^{-\frac{x-T}{aN_0}} dx + \mathbf{1}\{b < a\} e^{-\Lambda(T) - \frac{S}{aN_0}} \\ &= \frac{1}{2} (1 - e^{-\Lambda(T)}) + e^{-\Lambda(T)} \left[e^{-\frac{\delta \wedge S}{aN_0}} - e^{-\frac{S}{aN_0}} \right] + \mathbf{1}\{b < a\} e^{-\Lambda(T) - \frac{S}{aN_0}}, \end{aligned}$$

and

$$\begin{aligned} \mathbf{P}[\vartheta(X) = 2 \mid H_2] &= \frac{1}{2} \mathbf{P}[X < T \mid H_2] + \int_T^{T+S} \mathbf{1} \left\{ x < \frac{ab}{b-a} N_0 \log \frac{b}{a} + T \right\} f_2(x) dx \\ &\quad + \mathbf{1}\{a < b\} \mathbf{P}[X > T + S \mid H_2] \\ &= \frac{1}{2} (1 - e^{-\Lambda(T)}) + \int_T^{T+(\delta \wedge S)} e^{-\Lambda(T)} \frac{1}{bN_0} e^{-\frac{x-T}{bN_0}} dx + \mathbf{1}\{a < b\} e^{-\Lambda(T) - \frac{S}{bN_0}} \\ &= \frac{1}{2} (1 - e^{-\Lambda(T)}) + e^{-\Lambda(T)} \left[1 - e^{-\frac{\delta \wedge S}{bN_0}} \right] + \mathbf{1}\{a < b\} e^{-\Lambda(T) - \frac{S}{bN_0}}. \end{aligned}$$

Assuming equal prior probability of H_1 and H_2 we get

$$\mathbf{P}[\vartheta(X) = \vartheta] = \frac{1}{2} (1 - e^{-\Lambda(T)} + e^{-\Lambda(T) - \frac{S}{(a \vee b)N_0}})$$

$$\begin{aligned}
 & + \frac{1}{2}e^{-\Lambda(T)} \left[e^{-\frac{\delta\Lambda S}{aN_0}} - e^{-\frac{S}{aN_0}} \right] + \frac{1}{2}e^{-\Lambda(T)} \left[1 - e^{-\frac{\delta\Lambda S}{bN_0}} \right] \\
 & = \frac{1}{2} + \frac{1}{2}e^{-\Lambda(T)} \left(e^{-\frac{S}{(a\sqrt{b})N_0}} - e^{-\frac{S}{aN_0}} \right) + \frac{1}{2}e^{-\Lambda(T)} \left(e^{-\frac{\delta\Lambda S}{aN_0}} - e^{-\frac{\delta\Lambda S}{bN_0}} \right) \\
 & = \frac{1}{2} + \frac{1}{2}e^{-\Lambda(T)} \left(e^{-\frac{\delta\Lambda S}{aN_0}} - e^{-\frac{\delta\Lambda S}{bN_0}} \right).
 \end{aligned}$$

This assumed $a > b$. If instead $b > a$ then the inequalities in the integrand when we integrate between T and $T + S$ would be reversed, so the exact expression for any $a > 0, b > 0$ is

$$\mathbf{P}[\vartheta(X) = \vartheta] = \frac{1}{2} + \frac{1}{2}e^{-\Lambda(T)} \left(e^{-\frac{\delta\Lambda S}{(a\sqrt{b})N_0}} - e^{-\frac{\delta\Lambda S}{(a\sqrt{b})N_0}} \right). \tag{A.2}$$

□

Appendix B: Proof of Theorem 3.2

Proof. Fix an integer $J \geq 1$ and define $a_1 = a, a_2 = b$ for ease of notation. We first define the following auxiliary functions

$$\begin{aligned}
 Q_i(T) &\equiv e^{-\int_0^T \frac{dt}{N_i(t)}}, & Q_i(T, T+S) &\equiv e^{-\int_T^{T+S} \frac{dt}{N_i(t)}} \\
 q_i(T) &\equiv \frac{1}{N_i(T)} e^{-\int_0^T \frac{dt}{N_i(t)}}, & q_i(T, T+S) &\equiv \frac{1}{N_i(T+S)} e^{-\int_T^{T+S} \frac{dt}{N_i(t)}}
 \end{aligned}$$

The coalescent density for a coalescent time with effective population size trajectory N for the intervals $(0, T]$ and $(T + S, \infty)$ and N_i for the interval $(T, T + S]$ is

$$f_i(t) = \begin{cases} q(t) & 0 < t < T \\ Q(T)q_i(T, t) & T \leq t < T + S \\ Q(T)Q_i(T, T + S)q(T + S, t) & t \geq T + S \end{cases}$$

so that the likelihood ratio for a single time point can be expressed as

$$\begin{aligned}
 \frac{f_1(x^j)}{f_2(x^j)} &= \left[\frac{q_1(T, x^j)}{q_2(T, x^j)} \right]^{\mathbf{1}\{T \leq x^j < T+S\}} \left[\frac{Q_1(T, T+S)}{Q_2(T, T+S)} \right]^{\mathbf{1}\{x^j \geq T+S\}} \\
 &= \left[\frac{b}{a} e^{-\frac{(b-a)(x^j-T)}{abN_0}} \right]^{\mathbf{1}\{T \leq x^j < T+S\}} \left[e^{-S\frac{(b-a)}{abN_0}} \right]^{\mathbf{1}\{x^j \geq T+S\}},
 \end{aligned}$$

giving

$$\begin{aligned}
 \log \prod_{j=1}^J \frac{f_1(x^j)}{f_2(x^j)} &= \sum_{j=1}^J \mathbf{1}\{T < x^j \leq T + S\} \left[\log \frac{b}{a} - (x^j - T) \frac{(b-a)}{abN_0} \right] \\
 &\quad - \sum_{j=1}^J \mathbf{1}\{x^j > T + S\} \frac{S(b-a)}{abN_0}.
 \end{aligned}$$

Defining

$$\ell_1 = \sum_{j=1}^J \mathbf{1}\{x^j \leq T\}, \quad \ell_2 = \sum_{j=1}^J \mathbf{1}\{T < x^j \leq T + S\}, \quad \ell_3 = \sum_{j=1}^J \mathbf{1}\{x^j \geq T + S\},$$

we have that $\log \text{BF}_{12} > 0$ when

$$\begin{aligned} \sum_{j=1}^J \mathbf{1}\{T < x^j \leq T + S\} \left[\log \frac{b}{a} - (x^j - T) \frac{(b-a)}{abN_0} \right] &> \sum_{j=1}^J \mathbf{1}\{x^j > T + S\} \frac{S(b-a)}{abN_0} \\ \ell_2 \left(\log \frac{b}{a} + T \frac{(b-a)}{abN_0} \right) - \ell_3 S \frac{(b-a)}{abN_0} &> \frac{(b-a)}{abN_0} \sum_{j: x^j \in [T, T+S]} x^j \\ \ell_2 \left(\frac{abN_0}{a-b} \log \frac{a}{b} + T \right) - \ell_3 S &< \sum_{j: x^j \in [T, T+S]} x^j, \\ \ell_2 (\delta + T) - \ell_3 S &< \sum_{j: x^j \in [T, T+S]} x^j, \end{aligned}$$

where the inequality reversed since $(b-a)/(abN_0)$ is negative.

Now, $\log \text{BF}_{12} = 0$ only if $x^j < T$ for all $j = 1, \dots, J$. In this case, we flip a fair coin and accept H_1 if it shows heads. Moreover, if $L_2 = 0$ and $L_3 > 0$, then $\log \text{BF}_{12} > 0$. Denote by $L = (L_1, L_2, L_3)$ the random vector whose observed entries are $\ell = (\ell_1, \ell_2, \ell_3)$. Notice that for a generic coalescent time X

$$\begin{aligned} L \mid H_i &\sim \text{Multinomial}(J, \mathbf{p}) \\ p_1 &= \mathbf{P}[X \leq T] = (1 - e^{-\Lambda(T)}) \\ p_2 &= \mathbf{P}[T < X \leq T + S] = (e^{-\Lambda(T)} - e^{-\Lambda(T) - \frac{S}{a_i N_0}}) \\ p_3 &= \mathbf{P}[X > T + S] = e^{-\Lambda(T) - \frac{S}{a_i N_0}}, \end{aligned}$$

and we have

$$\begin{aligned} \mathbf{P}[\vartheta(X^J) = 1 \mid H_1] &= \frac{1}{2} \mathbf{P}(L_1 = J \mid H_1) + \mathbf{P}(L_2 = 0, L_3 > 0 \mid H_1) \\ &+ \sum_{(\ell_2, \ell_3): \ell_2 > 0} \mathbf{P}(L = \ell \mid H_1) \mathbf{P}(\text{BF}_{12}(X^J) > 0 \mid L = \ell, H_1) \end{aligned}$$

with

$$\begin{aligned} \mathbf{P}[\text{BF}_{12}(X^J) > 0 \mid L = \ell, H_1] &= \mathbf{P} \left[\sum_{j: X^j \in [T, T+S]} X^j > \ell_2(\delta + T) - \ell_3 S \mid L = \ell \right] \\ &= \mathbf{P} \left[\sum_{j: X^j \in [T, T+S]} X^j > \ell_2(\delta + T) - \ell_3 S \mid T < X^j \leq T + S \right] \\ &= \mathbf{P} \left[\sum_{j=1}^{\ell_2} X_*^j > \ell_2 \delta - \ell_3 S \mid X_*^j < S \right] \end{aligned}$$

for X_*^j independent exponential random variables with rate $(aN_0)^{-1}$. So letting $W^*(\ell_2) = \sum_{j=1}^{\ell_2} X_*^j$, the relevant probabilities involve the CDF of the sum of ℓ_2 many independent exponentials with rate $(aN_0)^{-1}$ truncated to the interval $[0, S]$, and we have

$$\begin{aligned} \mathbf{P}[\vartheta(X^J) = 1 \mid H_1] &= \frac{1}{2} \mathbf{P}(L_1 = J \mid H_1) + \mathbf{P}(L_2 = 0, L_3 > 0 \mid H_1) \\ &+ \sum_{(\ell_2, \ell_3): \ell_2 > 0} \mathbf{P}(L = \ell \mid H_1) \mathbf{P}[W^*(\ell_2) > \ell_2 \delta - \ell_3 S \mid H_1]. \end{aligned}$$

It follows then that since $\mathbf{P}(L_1 = J | H_1) = \mathbf{P}(L_1 = J | H_2)$, the Bayes error rate can be written as

$$\begin{aligned} \mathbf{P}[\vartheta(X^J) = \vartheta] &= \frac{1}{2} \mathbf{P}(L_2 = 0 | H_1) \\ &+ \frac{1}{2} \sum_{(\ell_2, \ell_3): \ell_2 > 0} \mathbf{P}(L = \ell | H_1) \mathbf{P}[W^*(\ell_2) > \ell_2 \delta - \ell_3 S | H_1] \\ &+ \frac{1}{2} \sum_{(\ell_2, \ell_3): \ell_2 > 0} \mathbf{P}(L = \ell | H_2) \mathbf{P}[W^*(\ell_2) < \ell_2 \delta - \ell_3 S | H_2]. \end{aligned} \tag{B.1}$$

□

Appendix C: Proof of Theorem 5.1

Recall we are studying the case where $H_1 : N = N_1(t)$ and $H_2 : N = N_2(t)$ and

$$N_1(t) = \begin{cases} N(t) & 0 \leq t \leq T \\ aN_0 & T \leq t \leq T + S \\ N(t) & t > T + S \end{cases}$$

$$N_2(t) = \begin{cases} N(t) & 0 \leq t \leq T \\ bN_0 & T \leq t \leq T + S \\ N(t) & t > T + S \end{cases}$$

for $N(t)$ any bounded, strictly non-negative function.

1. *Case 1:* $0 < x_2 < x_1 < T$. In this case the likelihood under either H_1 or H_2 is the same

$$L(x_2, x_1 | N(t)) = \frac{3}{N(x_2)N(x_1)} e^{-2\Lambda(x_2) - \Lambda(x_1)}$$

and so

$$\log \text{BF}_{12}(x) = 0.$$

2. *Case 2:* $0 < x_2 < T < x_1 < T + S$. In this case the likelihood under H_i is

$$L(x_2, x_1 | N(t)) = \frac{3}{N(x_2)} \frac{1}{a_i N_0} e^{-2\Lambda(x_2) - \Lambda(T) - \frac{x_1 - T}{a_i N_0}}$$

so designating $a_1 = a, a_2 = b$ as before

$$\begin{aligned} \log \text{BF}_{12}(x) &= \log \frac{b}{a} - \frac{x_1 - T}{aN_0} + \frac{x_1 - T}{bN_0} \\ &= \log \frac{b}{a} + \frac{(a - b)(x_1 - T)}{abN_0}. \end{aligned}$$

3. *Case 3:* $0 < x_2 < T < T + S < x_1$. In this case the likelihood under H_i is

$$L(x_2, x_1 | N(t)) = \frac{3}{N(x_2)} \frac{1}{N(x_1)} e^{-2\Lambda(x_2) - \Lambda(T) - \frac{S}{a_i N_0} - \Lambda(T + S, x_1)}$$

so

$$\log \text{BF}_{12}(x) = \frac{S}{bN_0} - \frac{S}{aN_0} = \frac{(a - b)S}{abN_0}.$$

4. *Case 4:* $0 < T < x_2 < x_1 < T + S$. In this case the likelihood under H_i is

$$\begin{aligned} L(x_2, x_1 \mid N(t)) &= \frac{3}{a_i N_0} \frac{1}{a_i N_0} e^{-3\Lambda(T) - \frac{3(x_2 - T)}{a_i N_0} - \frac{x_1 - x_2}{a_i N_0}} \\ &= \frac{3}{a_i^2 N_0^2} e^{-3\Lambda(T)} e^{-\frac{2x_2 + x_1 - 3T}{a_i N_0}} \end{aligned}$$

so

$$\begin{aligned} \log \text{BF}_{12}(x) &= 2 \log \frac{b}{a} - \frac{2x_2 + x_1 - 3T}{aN_0} + \frac{2x_2 + x_1 - 3T}{bN_0} \\ &= 2 \log \frac{b}{a} + \frac{(a-b)(2x_2 + x_1 - 3T)}{abN_0} \end{aligned}$$

5. *Case 5:* $0 < T < x_2 < T + S < x_1$. In this case the likelihood under H_i is

$$\begin{aligned} L(x_2, x_1 \mid N(t)) &= \frac{3}{a_i N_0} \frac{1}{N(x_1)} e^{-2\Lambda(T) - \frac{2(x_2 - T)}{a_i N_0} - \Lambda(T) - \frac{S}{a_i N_0} - \Lambda(T + S, x_1)} \\ &= \frac{3}{a_i N_0} \frac{1}{N(x_1)} e^{-3\Lambda(T) - \Lambda(T + S, x_1)} e^{-\frac{2(x_2 - T) + S}{a_i N_0}} \end{aligned}$$

so

$$\begin{aligned} \log \text{BF}_{12}(x) &= \log \frac{b}{a} - \frac{2(x_2 - T) + S}{aN_0} + \frac{2(x_2 - T) + S}{bN_0} \\ &= \log \frac{b}{a} + \frac{(a-b)(2(x_2 - T) + S)}{abN_0} \end{aligned}$$

6. *Case 6:* $0 < T < T + S < x_2 < x_1$. In this case the likelihood under H_i is

$$\begin{aligned} L(x_2, x_1 \mid N(t)) &= \frac{3}{N(x_2)} \frac{1}{N(x_1)} e^{-2\Lambda(T) - \frac{2S}{a_i N_0} - 2\Lambda(T + S, x_2) - \Lambda(T) - \frac{S}{a_i N_0} - \Lambda(T + S, x_1)} \\ &= \frac{3}{N(x_2)} \frac{1}{N(x_1)} e^{-3\Lambda(T) - 2\Lambda(T + S, x_2) - \Lambda(T + S, x_1)} e^{-\frac{3S}{a_i N_0}} \end{aligned}$$

so

$$\log \text{BF}_{12}(x) = -\frac{3S}{aN_0} + \frac{3S}{bN_0} = \frac{3(a-b)S}{abN_0}$$

$$\log \text{BF}_{12}(x) = \begin{cases} 0 & 0 < x_2 < x_1 < T \\ \log \frac{b}{a} + \frac{(a-b)(x_1 - T)}{abN_0} & 0 < x_2 < T < x_1 < T + S \\ \frac{(a-b)S}{abN_0} & 0 < x_2 < T < T + S < x_1 \\ 2 \log \frac{b}{a} + \frac{(a-b)(x_1 + 2x_2 - 3T)}{abN_0} & 0 < T < x_2 < x_1 < T + S \\ \log \frac{b}{a} + \frac{(a-b)(2x_2 - 2T + S)}{abN_0} & 0 < T < x_2 < T + S < x_1 \\ \frac{3(a-b)S}{abN_0} & 0 < T < T + S < x_2 < x_1 \end{cases}$$

We go line by line calculating the components of $\mathbf{P}[\vartheta(X) = \vartheta \mid H_1]$. Designate each of the six pieces of the expression by Q_j , $j = 1, 2, \dots, 6$.

$$Q_1 = \frac{1}{2} \mathbf{P}[X_1 < T] = \frac{1}{2} \int_0^T \int_{x_2}^T \frac{3}{N(x_2)N(x_1)} e^{-2\Lambda(x_2) - \Lambda(x_1)}$$

$$\begin{aligned}
 &= \frac{1}{2} \int_0^T (e^{-\Lambda(x_2)} - e^{-\Lambda(T)}) \frac{3}{N(x_2)} e^{-2\Lambda(x_2)} dx_2 \\
 &= \frac{1}{2} \int_0^T \frac{3}{N(x_2)} e^{-3\Lambda(x_2)} dx_2 - e^{-\Lambda(T)} \int_0^T \frac{3}{N(x_2)} e^{-2\Lambda(x_2)} dx_2 \\
 &= \frac{1}{2} \left(1 - e^{-3\Lambda(T)} - e^{-\Lambda(T)} \frac{3}{2} \int_0^T \frac{2}{N_1(x_2)} e^{-2\Lambda(x_2)} dx_2 \right) \\
 &= \frac{1}{2} \left(1 - e^{-3\Lambda(T)} - e^{-\Lambda(T)} \frac{3}{2} (1 - e^{-2\Lambda(T)}) \right) \\
 &= \frac{1}{2} + \frac{1}{4} e^{-3\Lambda(T)} - \frac{3}{4} e^{-\Lambda(T)}
 \end{aligned}$$

Now define

$$\delta = \frac{abN_0}{a-b} \log \frac{a}{b}$$

then we have

$$\begin{aligned}
 Q_2 &= \int_0^T \int_T^{T+S} \frac{3}{N(x_2)N(x_1)} e^{-2\Lambda(x_2)-\Lambda(x_1)} \mathbf{1} \left\{ \log \frac{b}{a} + \frac{(a-b)(x_1-T)}{abN_0} > 0 \right\} dx_1 dx_2 \\
 &= \int_0^T \int_{T+(\delta \wedge S)}^{T+S} \frac{3}{N(x_2)N(x_1)} e^{-2\Lambda(x_2)-\Lambda(x_1)} dx_1 dx_2 \\
 &= (e^{-\Lambda(T)-\frac{\delta \wedge S}{aN_0}} - e^{-\Lambda(T)-\frac{S}{aN_0}}) \frac{3}{2} \int_0^T \frac{2}{N(x_2)} e^{-2\Lambda(x_2)} dx_2 \\
 &= (e^{-\frac{\delta \wedge S}{aN_0}} - e^{-\frac{S}{aN_0}}) e^{-\Lambda(T)} \frac{3}{2} (1 - e^{-2\Lambda(T)})
 \end{aligned}$$

For case 3

$$\begin{aligned}
 Q_3 &= \mathbf{1}\{a > b\} \int_0^T \int_{T+S}^{\infty} \frac{3}{N(x_2)N(x_1)} e^{-2\Lambda(x_2)-\Lambda(x_1)} dx_1 dx_2 \\
 &= \mathbf{1}\{a > b\} e^{-\Lambda(T)-\frac{S}{aN_0}} \frac{3}{2} \int_0^T \frac{2}{N(x_2)} e^{-2\Lambda(x_2)} dx_2 \\
 &= \frac{3}{2} \mathbf{1}\{a > b\} e^{-\Lambda(T)-\frac{S}{aN_0}} (1 - e^{-2\Lambda(T)})
 \end{aligned}$$

Case 4

$$\begin{aligned}
 Q_4 &= \int_T^{T+S} \int_{x_2}^{T+S} \frac{3}{N(x_2)N(x_1)} e^{-2\Lambda(x_2)-\Lambda(x_1)} \mathbf{1} \{x_1 > T + 2(T - x_2 + \delta)\} dx_1 dx_2 \\
 &= \int_T^{T+S} \int_{x_2}^{T+S} \frac{3}{a^2 N_0^2} e^{-3\Lambda(T)} e^{-\frac{2x_2+x_1-3T}{aN_0}} \mathbf{1} \{x_1 > T + 2(T - x_2 + \delta)\} dx_1 dx_2.
 \end{aligned}$$

The inequalities

$$0 < T < x_2 < x_1 < T + S, \quad x_1 > T + 2(T - x_2 + \delta)$$

reduce to

$$\frac{2\delta}{3} < S < 2\delta, \quad \frac{1}{3}(3T + 2\delta) < x_1 < S + T, \quad \frac{1}{2}(3T - x_1 + 2\delta) < x_2 < x_1$$

or

$$S > 2\delta$$

and either

$$\frac{1}{3}(3T + 2\delta) < x_1 < T + 2\delta, \quad \frac{1}{2}(3T - x_1 + 2\delta) < x_2 < x_1$$

or

$$T + 2\delta < x_1 < S + T, \quad T < x_2 < x_1.$$

So then we can express Q_4 as

$$Q_4 = \begin{cases} 0 & S < \frac{2}{3}\delta \\ Q_{41} & \frac{2}{3}\delta < S < 2\delta \\ Q_{42} & S > 2\delta \end{cases}$$

where

$$\begin{aligned} Q_{41} &= \int_{\frac{1}{3}(3T+2\delta)}^{T+S} \int_{\frac{1}{2}(3T-x_1+2\delta)}^{x_1} \frac{3}{a^2 N_0^2} e^{-3\Lambda(T)} e^{-\frac{2x_2+x_1-3T}{aN_0}} dx_2 dx_1 \\ &= \frac{1}{2} e^{-3\Lambda(T)} \left(e^{-\frac{3S}{aN_0}} - e^{-\frac{2\delta}{aN_0}} \frac{aN_0 - 3S + 2\delta}{aN_0} \right) \end{aligned}$$

and

$$\begin{aligned} Q_{42} &= \int_{\frac{1}{3}(3T+2\delta)}^{T+2\delta} \int_{\frac{1}{2}(3T-x_1+2\delta)}^{x_1} \frac{3}{a^2 N_0^2} e^{-3\Lambda(T)} e^{-\frac{2x_2+x_1-3T}{aN_0}} dx_2 dx_1 \\ &\quad + \int_{T+2\delta}^{T+S} \int_T^{x_1} \frac{3}{a^2 N_0^2} e^{-3\Lambda(T)} e^{-\frac{2x_2+x_1-3T}{aN_0}} dx_2 dx_1 \\ &= \frac{1}{2} e^{-3\Lambda(T)} \left(e^{-\frac{6\delta}{aN_0}} + e^{-\frac{2\delta}{aN_0}} \frac{4\delta - aN_0}{aN_0} \right) \\ &\quad + \frac{1}{2} e^{-3\Lambda(T)} \left(e^{-\frac{3S}{aN_0}} - 3e^{-\frac{S}{aN_0}} - e^{-\frac{6\delta}{aN_0}} + 3e^{-\frac{2\delta}{aN_0}} \right) \\ &= \left(\frac{1}{2} e^{-3\Lambda(T)} \left(e^{-\frac{2\delta}{aN_0}} \left(\frac{4\delta}{aN_0} + 2 \right) + e^{-\frac{3S}{aN_0}} - 3e^{-\frac{S}{aN_0}} \right) \right) \end{aligned}$$

And now for case 5

$$\begin{aligned} Q_5 &= \int_T^{T+S} \int_{T+S}^{\infty} f_1(x_1, x_2) \mathbf{1} \left\{ \log \frac{b}{a} + \frac{(a-b)(2(x_2-T)+S)}{abN_0} > 0 \right\} dx_1 dx_2 \\ &= \int_T^{T+S} \int_{T+S}^{\infty} \frac{3}{N(x_2)N(x_1)} e^{-2\Lambda(x_2)-\Lambda(x_1)} \mathbf{1} \left\{ x_2 > T + \frac{\delta}{2} - \frac{S}{2} \right\} dx_1 dx_2 \\ &= \int_{T+\{0 \vee ((\frac{\delta}{2}-\frac{S}{2}) \wedge S)\}}^{T+S} \frac{3}{N(x_2)} e^{-2\Lambda(x_2)} dx_2 \int_{T+S}^{\infty} \frac{1}{N(x_1)} e^{-\Lambda(x_1)} dx_1 \\ &= \frac{3}{2} e^{-\Lambda(T)-\frac{S}{aN_0}} \int_{T+\{0 \vee ((\frac{\delta}{2}-\frac{S}{2}) \wedge S)\}}^{T+S} \frac{2}{N(x_2)} e^{-2\Lambda(x_2)} dx_2 \\ &= \frac{3}{2} e^{-\Lambda(T)-\frac{S}{aN_0}} (e^{-2\Lambda(T+\{0 \vee ((\frac{\delta}{2}-\frac{S}{2}) \wedge S)\})} - e^{-2\Lambda(T+S)}) \\ &= \frac{3}{2} e^{-3\Lambda(T)-\frac{S}{aN_0}} (e^{-\frac{2\{0 \vee ((\frac{\delta}{2}-\frac{S}{2}) \wedge S)\}}{aN_0}} - e^{-\frac{2S}{aN_0}}) \end{aligned}$$

Finally case 6

$$\begin{aligned} Q_6 &= \mathbf{1}\{a > b\} \int_{T+S}^{\infty} \int_{x_2}^{\infty} \frac{3}{N(x_2)N(x_1)} e^{-2\Lambda(x_2)-\Lambda(x_1)} dx_1 dx_2 \\ &= \mathbf{1}\{a > b\} \int_{T+S}^{\infty} \frac{3}{N(x_2)} e^{-3\Lambda(x_2)} dx_2 \\ &= \mathbf{1}\{a > b\} e^{-3\Lambda(T)-\frac{3S}{aN_0}} \end{aligned}$$

Now we can get the other component fairly easily. We repeat the calculations conditioning on H_2

$$Q_1 = \frac{1}{2} \left(1 + \frac{1}{2} e^{-3\Lambda(T)} - \frac{3}{2} e^{-\Lambda(T)} \right)$$

case 2

$$\begin{aligned} Q_2 &= \int_0^T \int_T^{T+S} \frac{3}{N(x_2)N(x_1)} e^{-2\Lambda(x_2)-\Lambda(x_1)} \mathbf{1} \left\{ \log \frac{b}{a} + \frac{(a-b)(x_1-T)}{abN_0} < 0 \right\} dx_1 dx_2 \\ &= \int_0^T \int_T^{T+(\delta \wedge S)} \frac{3}{N(x_2)N(x_1)} e^{-2\Lambda(x_2)-\Lambda(x_1)} dx_1 dx_2 \\ &= (e^{-\Lambda(T)} - e^{-\Lambda(T)-\frac{\delta \wedge S}{bN_0}}) \frac{3}{2} \int_0^T \frac{2}{N(x_2)} e^{-2\Lambda(x_2)} dx_2 \\ &= (1 - e^{-\frac{\delta \wedge S}{bN_0}}) e^{-\Lambda(T)} \frac{3}{2} (1 - e^{-2\Lambda(T)}) \end{aligned}$$

For case 3

$$\begin{aligned} Q_3 &= \mathbf{1}\{b > a\} \int_0^T \int_{T+S}^{\infty} \frac{3}{N(x_2)N(x_1)} e^{-2\Lambda(x_2)-\Lambda(x_1)} dx_1 dx_2 \\ &= 0 \end{aligned}$$

Case 4

$$\begin{aligned} Q_4 &= \int_T^{T+S} \int_{x_2}^{T+S} \frac{3}{N(x_2)N(x_1)} e^{-2\Lambda(x_2)-\Lambda(x_1)} \mathbf{1} \{x_1 < T + 2(T - x_2 + \delta)\} dx_1 dx_2 \\ &= \int_T^{T+S} \int_{x_2}^{T+S} \frac{3}{b^2 N_0^2} e^{-3\Lambda(T)} e^{-\frac{2x_2+x_1-3T}{bN_0}} \mathbf{1} \{x_1 < T + 2(T - x_2 + \delta)\} dx_1 dx_2. \end{aligned}$$

The inequalities

$$0 \leq T \leq x_2 \leq x_1 \leq T + S, \quad x_1 \leq T + 2(T - x_2 + \delta), \quad \delta > 0$$

reduce to

$$\begin{aligned} 0 \leq S \leq \frac{2\delta}{3}, \quad T \leq x_1 \leq S + T, \quad T \leq x_2 \leq x_1, \quad \text{or} \\ \frac{2\delta}{3} \leq S \leq 2\delta, \quad \begin{cases} T < x_1 \leq \frac{1}{3}(3T + 2\delta), & T \leq x_2 \leq x_1 \quad \text{or} \\ \frac{1}{3}(3T + 2\delta) \leq x_1 \leq T + S & T \leq x_2 \leq \frac{1}{2}(3T - x_1 + 2\delta) \end{cases} \end{aligned}$$

or

$$S > 2\delta, \quad \begin{cases} T < x_1 < \frac{1}{3}(3T + 2\delta), & T < x_2 < x_1 \quad \text{or} \\ \frac{1}{3}(3T + 2\delta) \leq x_1 \leq T + 2\delta, & T < x_2 \leq \frac{1}{2}(3T - x_1 + 2\delta) \end{cases}$$

so

$$Q_4 = \begin{cases} Q_{41} & 0 \leq S \leq \frac{2\delta}{3} \\ Q_{42} & \frac{2\delta}{3} \leq S \leq 2\delta, \\ Q_{43} & S > 2\delta \end{cases},$$

where

$$\begin{aligned} Q_{41} &= \frac{1}{2} e^{-3\Lambda(T)} \left(e^{-\frac{3S}{bN_0}} - 3e^{-\frac{S}{bN_0}} + 2 \right) \\ Q_{42} &= \frac{1}{2} e^{-3\Lambda(T)} \left(\frac{e^{-\frac{2\delta}{bN_0}} (bN_0 + 2\delta - 3S)}{bN_0} - 3e^{-\frac{S}{bN_0}} + 2 \right) \\ Q_{43} &= \frac{1}{2bN_0} e^{-3\Lambda(T)} e^{-\frac{2\delta+S}{bN_0}} \left(bN_0 \left(2e^{\frac{2\delta+S}{bN_0}} + e^{\frac{S}{bN_0}} - 3e^{\frac{T}{bN_0}} \right) + e^{\frac{S}{bN_0}} (-4\delta - 3S + 3T) \right) \end{aligned}$$

Case 5

$$\begin{aligned} Q_5 &= \int_T^{T+S} \int_{T+S}^{\infty} f_1(x_1, x_2) \mathbf{1} \left\{ \log \frac{b}{a} + \frac{(a-b)(2(x_2-T)+S)}{abN_0} < 0 \right\} dx_1 dx_2 \\ &= \int_T^{T+S} \int_{T+S}^{\infty} \frac{3}{N(x_2)N(x_1)} e^{-2\Lambda(x_2)-\Lambda(x_1)} \mathbf{1} \left\{ x_2 < T + \frac{\delta}{2} - \frac{S}{2} \right\} dx_1 dx_2 \\ &= \int_T^{T+\{0 \vee ((\frac{\delta}{2}-\frac{S}{2}) \wedge S)\}} \frac{3}{N(x_2)} e^{-2\Lambda(x_2)} dx_2 \int_{T+S}^{\infty} \frac{1}{N(x_1)} e^{-\Lambda(x_1)} dx_1 \\ &= \frac{3}{2} e^{-\Lambda(T)-\frac{S}{bN_0}} \int_T^{T+\{0 \vee ((\frac{\delta}{2}-\frac{S}{2}) \wedge S)\}} \frac{2}{N(x_2)} e^{-2\Lambda(x_2)} dx_2 \\ &= \frac{3}{2} e^{-\Lambda(T)-\frac{S}{bN_0}} (e^{-2\Lambda(T)} - e^{-2\Lambda(T+\{0 \vee ((\frac{\delta}{2}-\frac{S}{2}) \wedge S)\})}) \\ &= \frac{3}{2} e^{-3\Lambda(T)-\frac{S}{bN_0}} \left(1 - e^{-\frac{2\{0 \vee ((\frac{\delta}{2}-\frac{S}{2}) \wedge S)\}}{bN_0}} \right) \end{aligned}$$

Case 6

$$\begin{aligned} Q_6 &= \mathbf{1}\{b > a\} \int_{T+S}^{\infty} \int_{x_2}^{\infty} \frac{3}{N(x_2)} \frac{1}{N(x_1)} e^{-2\Lambda(x_2)-\Lambda(x_1)} dx_1 dx_2 \\ &= 0 \end{aligned}$$

Appendix D: Proof of theorem 7.1

Proof. Define $\Lambda_i(t) = \int_0^t \frac{1}{N_i(s)} ds$, we then have

$$\begin{aligned} \mathbf{P}[\vartheta(X) = 1 \mid H_1] &= \int_0^{\infty} \mathbf{1} \left\{ \left(\frac{1}{c} - 1 \right) \Lambda_1(x) > \log \frac{1}{c} \right\} \frac{1}{N_1(x)} e^{-\int_0^x \frac{1}{N_1(t)} dt} dx \\ &= \mathbf{P} \left[X > \Lambda_1^{-1} \left(\frac{c}{1-c} \log \frac{1}{c} \right) \mid H_1 \right] \\ &= e^{-\Lambda_1(\Lambda_1^{-1}(\frac{c}{1-c} \log \frac{1}{c}))} = e^{\frac{c \log c}{1-c}} \\ &= c^{\frac{c}{1-c}}, \end{aligned}$$

which implicitly assumed that $c < 1$. Similarly

$$\mathbf{P}[\vartheta(X) = 2 \mid H_2] = \int_0^{\infty} \mathbf{1} \left\{ \Lambda_2(x) - \Lambda_1(x) < \log \frac{N_1(x)}{N_2(x)} \right\} \frac{1}{N_2(x)} e^{-\int_0^x \frac{1}{N_2(t)} dt} dx$$

$$\begin{aligned}
 &= \int_0^\infty \mathbf{1}\{\Lambda_2(x)(c-1) > \log c\} \frac{1}{N_2(x)} e^{-\int_0^x \frac{1}{N_2(t)} dt} dx \\
 &= \mathbf{P}\left[X < \Lambda_2^{-1}\left(\frac{1}{c-1} \log c\right) \mid H_2\right] = 1 - e^{-\Lambda_2(\Lambda_2^{-1}(\frac{1}{c-1} \log c))} \\
 &= 1 - c^{\frac{1}{1-c}}
 \end{aligned}$$

so then

$$\mathbf{P}[\vartheta(X) = \vartheta] = \frac{1}{2} c^{\frac{c}{1-c}} + \frac{1}{2} \left(1 - c^{\frac{1}{1-c}}\right).$$

□

Appendix E: Proof of theorem 7.2

Proof. Define $\Lambda_i(t) = \int_0^t \frac{1}{N_i(s)} ds$ and notice that

$$\begin{aligned}
 \text{BF}_{12} &= \prod_{j=1}^J \frac{\frac{1}{N_1(x^j)} e^{-\int_0^{x^j} \frac{1}{N_1(t)} dt}}{\frac{1}{N_2(x^j)} e^{-\int_0^{x^j} \frac{1}{N_2(t)} dt}} = \prod_{j=1}^J \frac{N_2(x^j) e^{-\int_0^{x^j} \frac{1}{N_1(t)} dt}}{N_1(x^j) e^{-\int_0^{x^j} \frac{1}{N_2(t)} dt}} \\
 &= c^J e^{-\sum_{j=1}^J \Lambda_1(x^j) - \Lambda_2(x^j)} = c^J e^{-\sum_{j=1}^J \Lambda_1(x^j) (1 - \frac{1}{c})} \\
 \log \text{BF}_{12} &= J \log c - \left(1 - \frac{1}{c}\right) \sum_{j=1}^J \Lambda_1(x^j)
 \end{aligned}$$

so then

$$\begin{aligned}
 \mathbf{P}[\log \text{BF}_{12} > 0 \mid H_1] &= \mathbf{P}\left[J \log c > \left(1 - \frac{1}{c}\right) \sum_{j=1}^J \Lambda_1(X^j) \mid H_1\right] \\
 &= \mathbf{P}\left[\left(\frac{1}{c} - 1\right) \sum_{j=1}^J \Lambda_1(X^j) > J \log \frac{1}{c} \mid H_1\right] \\
 &= \mathbf{P}\left[\sum_{j=1}^J \Lambda_1(X^j) > J \frac{c}{1-c} \log \frac{1}{c} \mid H_1\right].
 \end{aligned}$$

Since

$$\mathbf{P}[\Lambda_1(X) > s \mid H_1] = \mathbf{P}[X > \Lambda_1^{-1}(s)] = e^{-s},$$

we have

$$\mathbf{P}[\log \text{BF}_{12} > 0 \mid H_1] = \mathbf{P}\left[W > J \frac{c}{1-c} \log \frac{1}{c}\right],$$

where W is the sum of J independent unit rate exponentials, so $W \sim \text{Gamma}(J, 1)$ and

$$\mathbf{P}[\log \text{BF}_{12} > 0 \mid H_1] = 1 - \frac{1}{\Gamma(J)} \gamma\left(J, J \frac{c}{1-c} \log \frac{1}{c}\right),$$

where $\gamma(\alpha, \beta)$ is the lower incomplete Gamma function. Similar calculations give us that

$$\begin{aligned} \mathbf{P}[\log \text{BF}_{12} < 0 \mid H_2] &= \mathbf{P}\left[J \log c < (c-1) \sum_{j=1}^J \Lambda_2(X^j) \mid H_2\right] \\ &= \mathbf{P}\left[\sum_{i=1}^J \Lambda_2(X^j) < J \frac{1}{c-1} \log c \mid H_2\right] \\ &= \mathbf{P}\left[W < J \frac{1}{c-1} \log c\right] \\ &= \frac{1}{\Gamma(J)} \gamma\left(J, J \frac{1}{c-1} \log c\right) \end{aligned}$$

giving us

$$\mathbf{P}[\vartheta(X^J) = \vartheta] = \frac{1}{2} \left(1 - \frac{1}{\Gamma(J)} \gamma\left(J, J \frac{c}{1-c} \log \frac{1}{c}\right) + \frac{1}{\Gamma(J)} \gamma\left(J, J \frac{1}{c-1} \log c\right)\right),$$

as claimed. \square

Appendix F: Proof of Theorem 8.1

We have

$$f_i(x) = \begin{cases} \frac{1}{N(x)} e^{-\int_0^x \frac{1}{N(t)} dt} & x < T \\ \frac{1}{a_i N_0} e^{-\int_0^T \frac{1}{N(t)} dt} e^{-\frac{x-T}{a_i N_0}} & T \leq x < T+S \\ \frac{1}{N(x)} e^{-\int_0^T \frac{1}{N(t)} dt} e^{-\frac{S}{a_i N_0}} e^{-\int_{T+S}^x \frac{1}{N(t)} dt} & T+S \leq x \end{cases} \quad (\text{F.1})$$

where $f_i(x)$ is the density of a single coalescent time under H_i . Define

$$\Delta_{12}(x) \equiv (\sqrt{f_1(x)} - \sqrt{f_2(x)})^2.$$

So now we calculate

$$\int (\sqrt{f_1(x)} - \sqrt{f_2(x)})^2 dx = \int_0^T \Delta_{12}(x) dx + \int_T^{T+S} \Delta_{12}(x) dx + \int_{T+S}^\infty \Delta_{12}(x) dx$$

clearly the first term on the right is zero so

$$\int \Delta_{12}(x) dx = \int_T^{T+S} \Delta_{12}(x) dx + \int_{T+S}^\infty \Delta_{12}(x) dx.$$

Observe

$$\begin{aligned} \int_T^{T+S} \Delta_{12}(x) dx &= \int_T^{T+S} \left(\frac{1}{\sqrt{aN_0}} e^{-\frac{1}{2} \int_0^T \frac{1}{N(t)} dt} e^{-\frac{1}{2} \frac{x-T}{aN_0}} - \frac{1}{\sqrt{bN_0}} e^{-\frac{1}{2} \int_0^T \frac{1}{N(t)} dt} e^{-\frac{1}{2} \frac{x-T}{bN_0}} \right)^2 dx \\ &= e^{-\int_0^T \frac{1}{N(t)} dt} \int_T^{T+S} \left(\frac{1}{\sqrt{aN_0}} e^{-\frac{1}{2} \frac{x-T}{aN_0}} - \frac{1}{\sqrt{bN_0}} e^{-\frac{1}{2} \frac{x-T}{bN_0}} \right)^2 dx, \end{aligned}$$

then

$$e^{\int_0^T \frac{1}{N(t)} dt} \int_T^{T+S} \Delta_{12}(x) dx = 2 - e^{-\frac{S}{aN_0}} - e^{-\frac{S}{bN_0}} - \frac{4b(1 - e^{-\frac{(a+b)S}{2abN_0}}) \sqrt{a}}{(a+b)\sqrt{b}}, \quad (\text{F.2})$$

and now

$$\begin{aligned}
 \int_{T+S}^{\infty} \Delta_{12}(x) dx &= \int_{T+S}^{\infty} \left(\frac{1}{\sqrt{N(x)}} e^{-\frac{1}{2} \int_0^T \frac{1}{N(t)} dt} e^{-\frac{1}{2} \frac{S}{aN_0}} e^{-\frac{1}{2} \int_{T+S}^x \frac{1}{N(t)} dt} \right. \\
 &\quad \left. - \frac{1}{\sqrt{N(x)}} e^{-\frac{1}{2} \int_0^T \frac{1}{N(t)} dt} e^{-\frac{1}{2} \frac{S}{bN_0}} e^{-\frac{1}{2} \int_{T+S}^x \frac{1}{N(t)} dt} \right)^2 dx \\
 &= \int \left(e^{-\frac{1}{2} \frac{S}{aN_0}} - e^{-\frac{1}{2} \frac{S}{bN_0}} \right)^2 \left(\frac{1}{\sqrt{N(x)}} e^{-\frac{1}{2} \int_0^T \frac{1}{N(t)} dt} e^{-\frac{1}{2} \int_{T+S}^x \frac{1}{N(t)} dt} \right)^2 dx \\
 &= \left(e^{-\frac{1}{2} \frac{S}{aN_0}} - e^{-\frac{1}{2} \frac{S}{bN_0}} \right)^2 e^{-\int_0^T \frac{1}{N(t)} dt} \int_{T+S}^{\infty} \frac{1}{N(x)} e^{-\int_{T+S}^x \frac{1}{N(t)} dt} dx \\
 &= \left(e^{-\frac{1}{2} \frac{S}{aN_0}} - e^{-\frac{1}{2} \frac{S}{bN_0}} \right)^2 e^{-\int_0^T \frac{1}{N(t)} dt} \left(-e^{-\int_{T+S}^x \frac{1}{N(t)} dt} \Big|_{T+S}^{\infty} \right) \\
 &= \left(e^{-\frac{1}{2} \frac{S}{aN_0}} - e^{-\frac{1}{2} \frac{S}{bN_0}} \right)^2 e^{-\int_0^T \frac{1}{N(t)} dt}
 \end{aligned}$$

and adding this to (F.2)

$$\begin{aligned}
 H^2(f_1, f_2) &= \int \Delta_{12}(x) dx = e^{-\int_0^T \frac{1}{N(t)} dt} \left(1 - e^{-\frac{(a+b)S}{2abN_0}} \right) \frac{(a+b-2\sqrt{ab})}{a+b} \\
 &= e^{-\int_0^T \frac{1}{N(t)} dt} \left(1 - e^{-\frac{(a+b)S}{2abN_0}} \right) \frac{(\sqrt{a}-\sqrt{b})^2}{a+b}, \tag{F.3}
 \end{aligned}$$

which is the same as the last displayed equation on Kim et al. [12, p 11].

References

- [1] Peter Beerli and Joseph Felsenstein. Maximum likelihood estimation of a migration matrix and effective population sizes in n subpopulations by using a coalescent approach. *Proceedings of the National Academy of Sciences*, 98(8):4563–4568, 2001.
- [2] A.J. Drummond, M.A. Suchard, D. Xie, and A. Rambaut. Bayesian phylogenetics with BEAUti and the BEAST 1.7. *Molecular Biology and Evolution*, 29:1969–1973, 2012.
- [3] Joseph Felsenstein. Accuracy of coalescent likelihood estimates: Do we need more sites, more sequences, or more loci? *Molecular Biology and Evolution*, 23(3):691–700, 2006.
- [4] Joseph Felsenstein and Allen G Rodrigo. Coalescent Approaches to HIV Population Genetics. In *The Evolution of HIV*, pages 233–272. Johns Hopkins University Press, 1999.
- [5] Qiaomei Fu, Cosimo Posth, Mateja Hajdinjak, Martin Petr, Swapan Mallick, Daniel Fernandes, Anja Furtwängler, Wolfgang Haak, Matthias Meyer, Alissa Mittnik, Birgit Nickel, Alexander Peltzer, Nadin Rohland, Viviane Slon, Sahra Talamo, Iosif Lazaridis, Mark Lipson, Iain Mathieson, Stephan Schiffels, Pontus Skoglund, Anatoly P. Derevianko, Nikolai Drozdov, Vyacheslav Slavinsky, Alexander Tsybankov, Renata Grifoni Cremonesi, Francesco Mallegni, Bernard Gély, Eligio Vacca, Manuel R. González Morales, Lawrence G. Straus, Christine Neugebauer-Maresch, Maria Teschler-Nicola, Silviu Constantin, Oana Teodora Moldovan, Stefano Benazzi, Marco Peresani, Donato Coppola, Martina Lari, Stefano Ricci, Annamaria Ronchitelli, Frédérique Valentin, Corinne Thevenet, Kurt Wehrberger, Dan Grigorescu, Hélène Rougier, Isabelle Crevecoeur, Damien Flas, Patrick Semal, Marcello A. Mannino, Christophe Cupillard, Hervé Bocherens, Nicholas J. Conard, Katerina Harvati, Vyacheslav Moiseyev, Dorothée G. Drucker, Jiří Svoboda, Michael P. Richards, David Caramelli, Ron Pinhasi, Janet Kelso, Nick Patterson, Johannes Krause, Svante Pääbo, and David Reich. The genetic history of ice age europe. *Nature*, 534:200–205, 2016. URL <http://dx.doi.org/10.1038/nature17993>.

- [6] Y X Fu and W H Li. Statistical tests of neutrality of mutations. *Genetics*, 133(3):693–709, 1993.
- [7] Feng Gao and Alon Keinan. Explosive genetic evidence for explosive human population growth. *Current Opinion in Genetics and Development*, 41(Supplement C):130 – 139, 2016. Genetics of human origin.
- [8] Lucie Gattepaille, Torsten Günther, and Mattias Jakobsson. Inferring past effective population size from distributions of coalescent times. *Genetics*, 2016. .
- [9] R C Griffiths and S Tavaré. Sampling theory for neutral alleles in a varying environment. *Philosophical Transactions of the Royal Society of London. Series B, Biological Sciences*, 344: 403–410, June 1994.
- [10] Robert C. Griffiths and Paul Marjoram. An ancestral recombination graph. In Peter Donnelly and Simon Tavaré, editors, *Progress in population genetics and human evolution*, volume 87 of *IMA Volumes in Mathematics and Its Applications*, pages 257–270. Springer Verlag, New York, 1997.
- [11] James C Iles, Jayna Raghwani, GL Abby Harrison, Jacques Pepin, Cyrille F Djoko, Ubald Tamoufe, Matthew LeBreton, Bradley S Schneider, Joseph N Fair, Felix M Tshala, Patrick K Kayembe, Jean Jacques Muyembe, Samuel Edidi-Basepeo, Nathan D Wolfe, Peter Simmonds, Paul Klenerman, and Oliver G Pybus. Phylogeography and epidemic history of hepatitis C virus genotype 4 in Africa. *Virology*, 464-465(100):233–243, 09 2014.
- [12] Junhyong Kim, Elchanan Mossel, Miklós Z Rácz, and Nathan Ross. Can one hear the shape of a population history? *Theoretical population biology*, 100:26–38, 2015.
- [13] John F. C. Kingman. The coalescent. *Stochastic Processes and Their Applications*, 13(3): 235–248, 1982.
- [14] M.K. Kuhner, J. Yamato, and J. Felsenstein. Estimating effective population size and mutation rate from sequence data using Metropolis-Hastings sampling. *Genetics*, 140(4):1421–1430, 1995.
- [15] Heng Li and Richard Durbin. Inference of human population history from individual whole-genome sequences. *Nature*, 475(7357):493–496, July 2011.
- [16] Paul Marjoram and Jeff Wall. Fast “coalescent” simulation. *BMC Genetics*, 7(1), 2006.
- [17] G. McVean and N. Cardin. Approximating the coalescent with recombination. *Philos Trans R Soc Lond B Biol Sci*, 360(1459):1387–1393, Jul 2005.
- [18] Simon Myers, Charles Fefferman, and Nick Patterson. Can one learn history from the allelic spectrum? *Theoretical Population Biology*, 73(3):342 – 348, 2008.
- [19] Julia A. Palacios, John Wakeley, and Sohini Ramachandran. Bayesian nonparametric inference of population size changes from sequential genealogies. *Genetics*, 201(1):281–304, 2015.
- [20] Anna Pluzhnikov and Peter Donnelly. Optimal sequencing strategies for surveying molecular genetic diversity. *Genetics*, 144:1247–1262, 1996.
- [21] Raazesh Sainudiin, Kevin Thornton, Jennifer Harlow, James Booth, Michael Stillman, Ruriko Yoshida, Robert Griffiths, Gil McVean, and Peter Donnelly. Experiments with the site frequency spectrum. *Bulletin of Mathematical Biology*, 73(4):829–872, 2011.
- [22] Stephan Schiffels and Richard Durbin. Inferring human population size and separation history from multiple genome sequences. *Nature Genetics*, 46(8):919–925, 2014.
- [23] Beth Shapiro, Alexei J. Drummond, Andrew Rambaut, Michael C. Wilson, Paul E. Matheus, Andrei V. Sher, Oliver G. Pybus, M. Thomas P. Gilbert, Ian Barnes, Jonas Binladen, Eske Willerslev, Anders J. Hansen, Gennady F. Baryshnikov, James A. Burns, Sergei Davydov, Jonathan C. Driver, Duane G. Froese, C. Richard Harington, Grant Keddie, and Pavel Kosintsev. Rise and fall of the Beringian steppe bison. *Science*, 306(5701):1561–1565, 2004.
- [24] Sara Sheehan, Kelley Harris, and Yun S. Song. Estimating variable effective population sizes from multiple genomes: A sequentially Markov conditional sampling distribution approach. *Genetics*, 194(3):647–662, 2013.
- [25] M. Slatkin and R.R. Hudson. Pairwise comparisons of mitochondrial DNA sequences in stable and exponentially growing populations. *Genetics*, 129(2):555–562, 1991.

- [26] Matthew Stephens and Peter Donnelly. Inference in molecular population genetics. *Journal of the Royal Statistical Society: Series B (Statistical Methodology)*, 62(4):605–635, 2000.
- [27] Jonathan Terhorst and Yun S. Song. Fundamental limits on the accuracy of demographic inference based on the sample frequency spectrum. *Proceedings of the National Academy of Sciences*, 112(25):7677–7682, 2015.
- [28] Jonathan Terhorst, John A. Kamm, and Yun S. Song. Robust and scalable inference of population history from hundreds of unphased whole genomes. *Nature Genetics*, 49:303–309, 2017.
- [29] Yi-Gang Tong, Wei-Feng Shi, LiuDi, Jun Qian, Long Liang, Xiao-Chen Bo, Jun Liu, Hong-Guang Ren, Hang Fan, Ming Ni, Yang Sun, Yuan Jin, Yue Teng, Zhen Li, David Kargbo, Foday Dafaie, Alex Kanu, Cheng-Chao Chen, Zhi-Heng Lan, Hui Jiang, Yang Luo, Hui-Jun Lu, Xiao-Guang Zhang, Fan Yang, Yi Hu, Yu-Xi Cao, Yong-Qiang Deng, Hao-Xiang Su, Yu Sun, Wen-Sen Liu, Zhuang Wang, Cheng-Yu Wang, Zhao-Yang Bu, Zhen-Dong Guo, Liu-Bo Zhang, Wei-Min Nie, Chang-Qing Bai, Chun-Hua Sun, Xiao-Ping An, Pei-Song Xu, Xiang-Li-Lan Zhang, Yong Huang, Zhi-Qiang Mi, Dong Yu, Hong-Wu Yao, Yong Feng, Zhi-Ping Xia, Xue-Xing Zheng, Song-Tao Yang, Bing Lu, Jia-Fu Jiang, Brima Kargbo, Fu-Chu He, George F. Gao, Wu-Chun Cao, and The China Mobile Laboratory Testing Team in Sierra Leone. Genetic diversity and evolutionary dynamics of Ebola virus in Sierra Lhateone. *Nature*, 524(7563):93–96, 2015.
- [30] John Wakeley. *Coalescent Theory: An Introduction*. Roberts & Company Publishers, June 2008.
- [31] John Wakeley and Ori Sargsyan. Extensions of the coalescent effective population size. *Genetics*, 181:341–345, 2009.